# Applications of Chiral Symmetry

Thesis by

Hooman Davoudiasl

In Partial Fulfillment of the Requirements

for the Degree of

Doctor of Philosophy

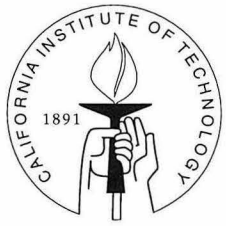


California Institute of Technology

Pasadena, California

1998

(Submitted April 24, 1998)

# Acknowledgements

Many people have contributed to the enrichment of my experiences while I have been at Caltech. First of all, I would like to thank Mark Wise, my Ph.D. advisor, scientific mentor, first collaborator, and tennis partner, not only for teaching me a great deal of physics and guiding me through my research, but also for doing so with a unique sense of humor. I would also like to thank my other collaborators, Adam Leibovich, Krishna Rajagopal, and Eric Westphal.

Over the past few years, I have benefited considerably from my interactions with David Beckman, Peter Cho, John Elwood, Steven Frautschi, Zoltan Ligeti, Stephen Ouellette, David Politzer, Costin Popescu, John Preskill, and John Schwarz. It is a pleasure to thank Helen Tuck who, with great competence and in impeccable style, has kept the business of our theory group in order and provided friendly support whenever needed.

I feel indebted to many good friends, Mina Aganagic, Paul Carter, Sergey Cherkis, Martin Gremm, Anton Kapustin, Yuri Levin, Krishna Rajagopal, Iain and Susan Stewart, Eric Westphal, and Patricia Wrean, who at numerous times offered me their help when I needed it, and made my life at Caltech more interesting and enjoyable, each in his or her own special way, but mostly through their humanity and friendship.

Finally, more than my words can say, I owe gratitude to my mother and grandmother who raised me with a great deal of dignity, and taught me much of what is important in life. They have given me so much, and asked for nothing. To say that I remember, I dedicate this work to them.

# Abstract

We study some applications of the chiral symmetry of quantum chromodynamics in treating phenomena involving hadrons at low energies, where perturbative methods are not valid. We begin by introducing the concepts of global symmetry breaking and the consequent generation of Goldstone bosons. It is shown how these concepts are realized through chiral symmetry breaking and provide an understanding of some of the features of strong interactions at low energies. This leads us to the chiral perturbation theory effective Lagrangian for the low energy interactions of the light pseudo-scalars. We use this effective Lagrangian, and the considerations that led to it, as the basis of our approach in studying three different problems. First, we find the rates for the $\tau$ lepton decays $\tau \to V\pi\nu_\tau$, where $V$ stands for $\rho$, $K^*$, or $\omega$, and extract the magnitude of the $\rho\,\omega\,\pi$ coupling, $\left|g_2^{(\rho)}\right| = 0.6$. Next, we use this coupling to find the decay rate for $D^0 \to \bar{K}^{*0}\pi^- e^+\nu_e$, in a certain kinematic regime. This rate depends on the $DD^*\pi$ coupling and our results can provide an extraction of this coupling, given data on this decay. The third problem we address is that of finding solutions that represent the qualitative behavior of the disoriented chiral condensate in the non-linear sigma model at $\mathcal{O}(p^4)$. We show that these solutions do not become singular at short distances where the $\mathcal{O}(p^2)$ solutions begin to diverge.

# Contents

# List of Figures

# Chapter 1 Introduction

*And now I will unclasp a secret book,*
*And to your quick-conceiving discontents*
*I'll read you matter deep and dangerous;*
*As full of peril and adventurous spirit*
*As to o'er-walk a current roaring loud*
*On the unsteadfast footing of a spear.* [1]

The concept of symmetry has played a central role in the progress of modern physics. Applications of symmetry have unified our understanding of various physical phenomena, enabling us to study nature fundamentally and quantitatively. The use of local symmetries has resulted in the invention of gauge theories which in turn have made it possible to perform numerous high precision and predictive computations. These computations are usually carried out in the context of a perturbative approach. For example, in quantum electrodynamics, perturbation theory provides highly precise means of calculating many physical quantities over a wide range of energies, and agreement between theoretical calculations and experimental results is remarkable.

However, perturbation theory is not always successful and has its limitations, as in quantum chromodynamics (QCD) which is the theory of strong interactions. At high energies, QCD is an asymptotically free theory [2, 3], perturbative calculations are valid, and agreement between theory and experiment is very good. However, QCD becomes a strongly interacting theory at energies comparable to or smaller than a typical energy scale, denoted by $\Lambda_{QCD} \sim 300$ MeV. For such energies, perturbative expansions break down, as the coupling constant $\alpha_s$ of the theory becomes large, $\alpha_s \sim 1$. In the regime where perturbation theory becomes unreliable, one must find other approaches for obtaining information on the behavior of the theory and its correspondence with data. In general, one must look for additional, and perhaps

approximate, symmetries of the theory.

A class of symmetries that are important in understanding physical phenomena are the global ones which, unlike gauge symmetries, are space-time independent. For example, baryon number conservation in strong interactions is a consequence of a symmetry that leaves the QCD Lagrangian invariant under a global $U_B(1)$ transformation of the quark fields. Another important global symmetry is the $SU(N_f)_L \times SU(N_f)_R$ chiral symmetry of the tree level QCD Lagrangian with $N_f$ massless quark flavors. This symmetry leaves such a Lagrangian invariant under separate global $SU(N_f)_L$ and $SU(N_f)_R$ transformations of the left-handed and the right-handed quark fields, respectively. However, the physical world contains only massive quarks and $SU(N_f)_L \times SU(N_f)_R$ is not an exact symmetry of QCD, at the tree level. This symmetry is also broken dynamically as the quark bilinear $\langle 0|\bar{q}^i q_j|0\rangle$ becomes non-zero at energies comparable to $\Lambda_{QCD}$.

Just as studying symmetries can yield useful information about a physical system, identifying broken and inexact symmetries, as well as finding mechanisms for symmetry breaking in a theory, can also provide us with significant insight into the fundamental principles that govern physical phenomena. For example, the breaking of the local $SU(2) \times U(1)$ electroweak symmetry via the Higgs mechanism has provided the Standard Model with a possible, although as yet experimentally unconfirmed, explanation for the behavior of the weak and electromagnetic interactions in a unified context [4].

Global symmetry breaking, accompanied by the generation of massless Goldstone bosons [5], has also been central to our understanding of many phenomena and led to the discovery of local symmetry breaking or the Higgs mechanism. The breaking of $SU(N_f)_L \times SU(N_f)_R$ chiral symmetry of the QCD Lagrangian is an important example of global symmetry breaking, and has various applications in studying the low energy strong interactions of hadrons. If quarks were massless, the dynamical breaking of chiral symmetry would result in the appearance of massless Goldstone bosons. However, quark masses break chiral symmetry, making the symmetry approximate for light flavors, at the tree level. Thus, the Goldstone bosons of the theory, the

pions in the case of two light quarks, are only approximately massless and are light compared to the scale of symmetry breaking $\Lambda_{\chi B} \sim 1$ GeV. The original application of these ideas in hadronic physics was in studying pion interactions, at energies small compared to $\Lambda_{\chi B}$, via the chiral perturbation theory effective Lagrangian. However, chiral Lagrangians have also been used in studying the coupling of light mesons, that is the pseudo-Goldstone bosons, to heavy matter fields such as baryons [6] and heavy mesons containing a heavy charm or bottom quark [7]. In the case of the heavy mesons, an extra approximate symmetry of the QCD Lagrangian, the heavy quark spin-flavor symmetry [8], has been incorporated into the effective chiral Lagrangian that is used in studying the coupling of the pseudo-Goldstone bosons with the heavy mesons.

In this work, we study the applications of chiral symmetry in low energy hadronic physics and present various contexts where effective Lagrangians based on this broken symmetry can be used to understand a variety of phenomena. These applications include calculating the rates for some hadronic decays of the $\tau$ lepton [9] and a semileptonic decay of the $D^0$ meson [10], and finding solutions for the conjectured domains of Disoriented Chiral Condensate (DCC) in heavy ion collisions [11]. Chapters 3, 4, and 5 are fairly self-contained in their discussion of the particular application of chiral symmetry that they present. However, we also discuss some general concepts and formalism related to chiral symmetry in strong interactions; this is the subject of the next chapter.

# Chapter 2 Chiral Symmetry: Concepts and Formalism

## 2.1 Spontaneous Global Symmetry Breaking and Goldstone Bosons

In this section, we study the spontaneous breaking of a global symmetry and its generic features in a toy model. Later, we study these basic ideas in the context of a more physically motivated Lagrangian that can be used to describe the low energy interactions of the eight lightest pseudo-scalar mesons. This will lead us to the effective Lagrangian of Chiral Perturbation Theory which is used as the basis of our approach to the description of low energy hadronic processes in the following chapters.

To start, let us examine the following Lagrangian for the complex scalar field $\phi$ [12]

$$\mathcal{L} = \partial_\mu \phi^* \, \partial^\mu \phi - m^2 \phi^* \, \phi - \lambda (\phi^* \, \phi)^2. \tag{2.1}$$

In the above equation, $m^2$ is considered to be a parameter and is not necessarily the mass squared of the field $\phi$, since we take $m^2 < 0$ later on. The parameter $\lambda$ is the self-coupling constant. We note that the Lagrangian $\mathcal{L}$ is invariant under a global $U(1)$ transformation

$$\phi \to e^{i\alpha} \, \phi, \tag{2.2}$$

where $\alpha$ is an arbitrary real constant.

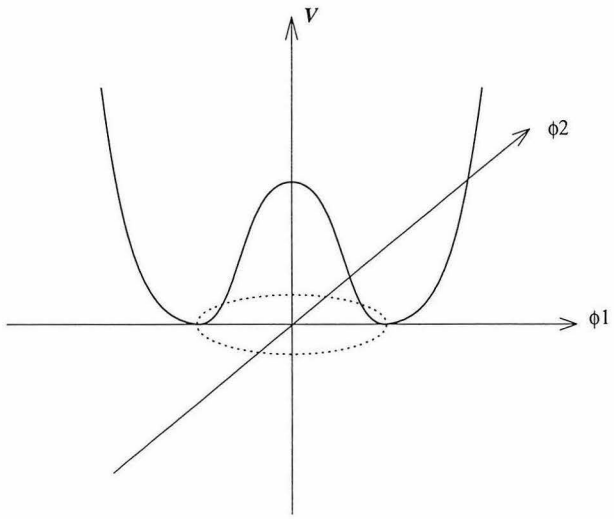


Figure 2.1: The potential of the Lagrangian (2.1). The circle represents the degenerate vacua of the theory.

The potential is given by

$$V(\phi) = m^2 \phi^* \phi + \lambda(\phi^* \phi)^2, \tag{2.3}$$

and the ground state, that is the vacuum of the theory, is obtained by minimizing the potential

$$\frac{\partial V}{\partial \phi} = m^2 \phi^* + 2\lambda \phi^* (\phi^* \phi) = 0. \tag{2.4}$$

Eq. (2.4) has a trivial solution $\phi = 0$ which for $m^2 > 0$ gives the minimum of $V(\phi)$. However, if $m^2 < 0$ the local maximum of $V(\phi)$ is given by $\phi = 0$ and the local minimum occurs at

$$|\phi|^2 = \frac{-m^2}{2\lambda} = v^2 \ ; \ v \in R. \tag{2.5}$$

The solution at $|\phi| = v$ is identified with the vacuum expectation value (vev) of the field $\phi$ in a quantum field theory description, $\langle 0|\phi|0\rangle = v$. This solution corresponds to a circle of radius $v$ in coordinates $\phi_1$ and $\phi_2$, where $\phi = \phi_1 + i\phi_2$, as shown in Fig. (2.1). This circle represents the degenerate vacua that are related by rotations.

The excitations above the vacuum, corresponding to the physical fields, are then given by perturbations about $|\phi| = v$ and not $|\phi| = 0$. It is instructive to parameterize the field $\phi$ in terms of two real fields $\chi(x)$ and $\theta(x)$

$$\phi(x) = \chi(x)\, e^{i\theta(x)}, \tag{2.6}$$

where $\langle 0|\chi(x)|0\rangle = v$ and $\langle 0|\theta(x)|0\rangle = 0$, for a particular choice of the vacuum $\langle 0|\phi(x)|0\rangle = v$. Thus, by fixing the vev's, we have removed the invariance of the vacuum under the $U(1)$ rotations. We also define the field $\tilde{\chi}(x)$ by

$$\phi(x) = [v + \tilde{\chi}(x)]\, e^{i\theta(x)}, \tag{2.7}$$

where $\langle 0|\tilde{\chi}(x)|0\rangle = 0$. Substituting for $\phi(x)$ in Eq. (2.1) from Eq. (2.7), we get

$$\mathcal{L} = \partial_\mu \tilde{\chi}\, \partial^\mu \tilde{\chi} + (v + \tilde{\chi})^2 \partial_\mu \theta\, \partial^\mu \theta - m^2 (v + \tilde{\chi})^2 - \lambda (v + \tilde{\chi})^4. \tag{2.8}$$

The coefficient of the term quadratic in $\tilde{\chi}$ in the Lagrangian (2.8) gives the mass $m_{\tilde{\chi}}$ of the $\tilde{\chi}$ particle

$$m_{\tilde{\chi}}^2 = 4\lambda v^2, \tag{2.9}$$

where we have used Eq. (2.5) to eliminate $m^2$. However, the Lagrangian (2.8) contains no quadratic terms in $\theta$ and, therefore, $\theta$ represents a massless particle in our theory. We observe that, starting from a theory that has a $U(1)$ symmetry, by spontaneous symmetry breaking, we have ended up with a massless $\theta$ particle. This is a general phenomenon, that is, the spontaneous breaking of a continuous global symmetry results in the generation of one or more massless scalar fields. The above statement is the content of Goldstone's theorem, and such massless scalars are known as Goldstone bosons[1].

[1] In supersymmetric theories, the spontaneous breaking of supersymmetry generates spin-(1/2) Goldstone fermions.

## 2.2 Chiral Symmetry in QCD

Now that we have studied the consequences of spontaneous global symmetry breaking in a toy model, we will direct our attention to strong interactions and QCD, and will try to understand some of the physical phenomena involving hadrons in the context of global symmetries of the QCD Lagrangian. For $N_f$ flavors of quarks with masses $m^j$ ($j = 1, 2, \cdots, N_f$), the QCD Lagrangian is given by

$$\mathcal{L}_{QCD} = -\frac{1}{2}\mathrm{Tr}(G_{\mu\nu}G^{\mu\nu}) + \sum_{j=1}^{N_f} [i\,\bar{q}_L^j \gamma^\mu D_\mu q_L^j + i\,\bar{q}_R^j \gamma^\mu D_\mu q_R^j - \bar{q}_L^j m^j q_R^j - \bar{q}_R^j m^j q_L^j]. \tag{2.10}$$

Here, $D_\mu$ is the covariant derivative and is given by

$$i\,D_\mu = i\,\partial_\mu - g_s A_\mu^a T^a, \tag{2.11}$$

where $g_s$ is the strong interactions coupling constant, $A_\mu^a$ is the gluon field ($a = 1, 2, \cdots, 8$), and $T^a$ is a generator in the adjoint representation of the $SU(3)_c$ color gauge group; we have $\mathrm{Tr}(T^a T^b) = \frac{1}{2}\delta^{ab}$. The $SU(3)_c$ field strength tensor $G_{\mu\nu}$ is defined by

$$G_{\mu\nu} = \partial_\mu A_\nu - \partial_\nu A_\mu - g_s[A_\mu,\, A_\nu], \tag{2.12}$$

where $A_\mu = A_\mu^a T^a$.

If we set the quark masses to zero, that is taking $m^j = 0$, the quark sector of the Lagrangian (2.10) becomes

$$\mathcal{L}_{QCD}^{(q)} = i \sum_{j=1}^{N_f} [\bar{q}_L^j \gamma^\mu D_\mu q_L^j + \bar{q}_R^j \gamma^\mu D_\mu q_R^j]. \tag{2.13}$$

We see that $\mathcal{L}_{QCD}^{(q)}$ is invariant under chiral $SU(N_f)_L \times SU(N_f)_R$ transformations[2].

[2]Classically, the Lagrangian (2.13) has a $U(N_f)_L \times U(N_f)_R$ symmetry. However, quantum mechanical effects break the $U(1)_A$ axial symmetry. Thus, apart from the chiral $SU(N_f)_L \times SU(N_f)_R$symmetry, there remains a $U(1)_B$ symmetry that corresponds to the conservation of baryon

That is, $\mathcal{L}^{(q)}_{QCD}$ is invariant under separate $N_f$-dimensional rotations of the form

$$q \xrightarrow{SU(N_f)} \exp\left(i\sum_a \lambda^a \alpha_a\right) q, \tag{2.14}$$

of $q_L$ and $q_R$, where $\lambda^a$, $a = 1, 2, \cdots, N_f^2 - 1$, are the generators of $SU(N_f)$ in the fundamental representation and $\alpha_a$ are the rotation parameters. The $\lambda^a$ obey the commutation relation $[\lambda^a, \lambda^b] = 2if^{abc}\lambda^c$, where $f^{abc}$ are the structure constants. For example, for $N_f = 3$ massless quarks, $\lambda^a$ correspond to the Gell-Mann matrices, and $a = 1, 2, \cdots, 8$. Since the up, the down, and the strange quarks are light relative to the hadronic scale of 1 GeV, we may expect $SU(3)_L \times SU(3)_R$ to be an approximate symmetry of nature. However, the hadronic spectrum does not contain degenerate multiplets with opposite parity [13], as the symmetry would imply, although hadrons can be classified in $SU(3)_V = SU(3)_{L+R}$ multiplets. We also note that the octet of pseudo-scalar mesons are much lighter than other hadrons.

These experimental facts suggest that the vacuum of the theory does not have the symmetries of the classical Lagrangian, and that chiral $SU(3)_L \times SU(3)_R$ is spontaneously broken. Then, by Goldstone's theorem, we expect to observe massless modes corresponding to each broken symmetry generator. As mentioned before, the smallness of the $(u, d, s)$ quark masses suggest that the explicit symmetry breaking due to the mass terms of the form $m(\bar{q}_L q_R + \bar{q}_R q_L)$ is not severe in the $(u, d, s)$ sector. However, since the masses of these quarks are non-zero, we expect the generated Goldstone bosons to be light compared to the typical hadronic scale of order 1 GeV. These are the eight lightest pseudo-scalar mesons, corresponding to the eight broken generators after spontaneous chiral symmetry breaking; $SU(3)_L \times SU(3)_R \to SU(3)_V$. To find the order parameter for this symmetry breaking, we consider the Noether currents $J^{\mu\, a}_\chi$ associated with the symmetry group $SU(3)_L \times SU(3)_R$

$$J^{\mu\, a}_\chi = \bar{q}_\chi \gamma^\mu \frac{\lambda^a}{2} q_\chi, \tag{2.15}$$

number in strong interactions.

where $a = 1, 2, \cdots, 8$ and $\chi = L, R$.

Associated with $J^{\mu\, a}_{\chi}$ are the charges $Q^a_\chi$ given by

$$Q^a_\chi = \int d^3x J^{0\, a}_{\chi}(x), \tag{2.16}$$

and we have

$$[Q^a_{\chi_1}, Q^b_{\chi_2}] = i\, \delta_{\chi_1\chi_2}\, f^{abc} Q^c_{\chi_1}. \tag{2.17}$$

Since the ground state of the theory in strong interactions is not invariant under the chiral group $SU(3)_L \times SU(3)_R$, we have

$$\langle 0|[Q^a_A, O^b]|0\rangle \neq 0, \tag{2.18}$$

where $Q^a_A = Q^a_R - Q^a_L$ are the axial charge operators, and $O^b = \bar{q}\gamma_5\lambda^b q$ are the operators representing the light pseudo-scalars. The quantity on the left-hand side of Eq. (2.18) is the symmetry breaking order parameter. We have [13],

$$\langle 0|[Q^a_A, O^b]|0\rangle = \langle 0|[Q^a_A, \bar{q}\gamma_5\lambda^b q]|0\rangle = -\frac{2}{3}\delta^{ab}\langle 0|\bar{q}q|0\rangle, \tag{2.19}$$

where we have used $\{\lambda^a, \lambda^b\} = (4/3)\delta^{ab} + 2d^{abc}\lambda^c$; $d^{abc}$ are totally symmetric coefficients. Note that we have $\langle 0|\bar{q}\lambda^c q|0\rangle = 0$. From Eq. (2.19) we see that the order parameter for chiral symmetry breaking is the quark condensate $\langle\bar{q}q\rangle \equiv \langle 0|\bar{q}q|0\rangle$. Therefore, as the quark bilinear dynamically gets a non-zero vev, that is $\langle\bar{u}u\rangle = \langle\bar{d}d\rangle = \langle\bar{s}s\rangle \neq 0$, chiral symmetry becomes broken, resulting in the appearance of the octet of light mesons $\pi^+, \pi^-, \pi^0, K^+, K^-, K^0, \bar{K}^0$, and $\eta$, which are the pseudo-Goldstone bosons of our theory.

In the next section, we will show how the interactions of the pseudo-Goldstone bosons can be formulated in terms of an effective Lagrangian that incorporates the features of the QCD Lagrangian that were discussed above. This will lead us to a perturbative expansion in powers of momenta for low energy hadronic interactions,

known as Chiral Perturbation Theory.

## 2.3 Chiral Perturbation Theory

The spontaneous breaking of chiral symmetry is understood in terms of the dynamical generation of a non-zero vev for the scalar quark density $v \equiv \langle \bar{q}q \rangle$. In $SU(3)_L \times SU(3)_R$, $q$ is one of the $(u, d, s)$ quarks. Later, we will show that the energy scale of chiral symmetry breaking is about 1 GeV. Thus, we note here that the approximate chiral symmetry of the QCD Lagrangian is enhanced if one considers the up and the down quark sector only, since the masses of these quarks are much smaller than the strange quark mass; $m_{u,d} \sim 10$ MeV, $m_s \sim 100$ MeV. For the $(u, d)$ sector, we have an $SU(2)_L \times SU(2)_R$ chiral symmetry, and the resulting pseudo-Goldstone bosons are $\pi^+, \pi^-$, and $\pi^0$. The calculations of the following chapters only require the $SU(2)_L \times SU(2)_R$ chiral symmetry. However, in this section, we consider the strange quark to be light and present the effective $SU(3)_L \times SU(3)_R$ chiral Lagrangian from which the $SU(2)_L \times SU(2)_R$ Lagrangian can easily be obtained.

We begin by studying the transformation properties of the quark condensate $\langle \bar{q}_{jR}(x)\, q_{kL}(x) \rangle$ under chiral rotations. We write

$$\langle \bar{q}_{jR}(x)\, q_{kL}(x) \rangle = v\delta_{jk}, \tag{2.20}$$

imposing the condition $j = k$, because an electromagnetically charged condensate breaks the electromagnetic gauge invariance. Separate chiral rotations of the left- and the right-handed quarks give

$$\langle \bar{q}_{jR}\, q_{kL} \rangle \to R^*_{jm} L_{kn} \langle \bar{q}_{mR}\, q_{nL} \rangle = v R^*_{jm} L_{kn} \delta_{mn} = v(LR^\dagger)_{kj}, \tag{2.21}$$

where $L \in SU(3)_L$ and $R \in SU(3)_R$. Thus, we see that the quark condensate is invariant under $SU(3)_V$, for which $L = R$.

The pseudo-Goldstone bosons correspond to excitations over the quark conden-

sate. We denote these excitations, that is the eight light mesons, by $\Sigma$,

$$\Sigma_{kj}(x) \sim \frac{1}{v}\langle \bar{q}_{jR}\, q_{kL}\rangle(x). \tag{2.22}$$

By analogy with the chiral transformations of $\langle \bar{q}_{jR}\, q_{kL}\rangle$ in Eq. (2.21), we require that

$$\Sigma \to L\Sigma R^{\dagger}, \tag{2.23}$$

under $SU(3)_L \times SU(3)_R$.

It is convenient to incorporate the meson fields into a matrix $M$ that is given by

$$M = \begin{bmatrix} \frac{1}{\sqrt{2}}\pi^0 + \frac{1}{\sqrt{6}}\eta & \pi^+ & K^+ \\ \pi^- & -\frac{1}{\sqrt{2}}\pi^0 + \frac{1}{\sqrt{6}}\eta & K^0 \\ K^- & \bar{K}^0 & -\sqrt{\frac{2}{3}}\eta \end{bmatrix}. \tag{2.24}$$

In analogy with the polar representation used in Section 2.1 to denote the massless Goldstone field, we define the field $\Sigma$ by

$$\Sigma = e^{(2iM/f)}, \tag{2.25}$$

where $f$ is some constant of mass dimension 1 that will be interpreted later.

Since we are interested in the low energy regime of hadronic interactions, we construct the effective chiral Lagrangian for the light pseudo-scalars from a minimum number of derivatives. From Lorentz invariance, each term in the Lagrangian must have an even number of derivatives. In the chiral limit, where the quark masses are zero, the pseudo-Goldstone bosons, which are the mesons, are massless. Thus, in that limit, the minimum number of derivatives at the lowest order is two. The lowest order effective chiral Lagrangian, invariant under $SU(3)_L \times SU(3)_R$, is then given by

$$\mathcal{L}_I^{(2)} = \frac{f^2}{8}\mathrm{Tr}\left(\partial_\mu \Sigma^{\dagger}\, \partial^\mu \Sigma\right), \tag{2.26}$$

where $\Sigma \to L\Sigma R^{\dagger}$, under chiral transformations.

To incorporate explicit chiral symmetry breaking due to the non-zero masses of quarks, we need terms proportional to the $(u, d, s)$ quark masses

$$\mathcal{L}_{II}^{(2)} = v\mathrm{Tr}\left(m_q\Sigma + m_q\Sigma^\dagger\right), \tag{2.27}$$

where $v$ is a constant of mass dimension 3 and $m_q$ is the quark mass matrix

$$m_q = \begin{bmatrix} m_u & 0 & 0 \\ 0 & m_d & 0 \\ 0 & 0 & m_s \end{bmatrix}. \tag{2.28}$$

Note that since $\Sigma \to L\Sigma R^\dagger$ under $SU(3)_L \times SU(3)_R$ rotations, the terms in Eq. (2.27) transform like the mass terms in the QCD Lagrangian, under chiral rotations.

The mass terms for the mesons are included in $\mathcal{L}_{II}^{(2)}$. We thus treat the terms in $\mathcal{L}_{II}^{(2)}$ as being at the same order as the two-derivative terms, because the masses of the mesons $m_M \sim p$, where $p \ll \Lambda_{\chi B}$ is a typical momentum scale for low energy interactions of the mesons. Therefore, the effective Lagrangian for the light pseudoscalar meson interactions at the leading order in a derivative expansion is given by

$$\mathcal{L}^{(2)} = \mathcal{L}_I^{(2)} + \mathcal{L}_{II}^{(2)}. \tag{2.29}$$

Henceforth, we refer to the order of chiral Lagrangians by the highest power of momentum they include. Thus, the above Lagrangian is $\mathcal{O}(p^2)$, and the next to leading order Lagrangian is $\mathcal{O}(p^4)$, and so on.

We can derive the mass terms for the mesons in terms of $v$ and $f$, using $\mathcal{L}_{II}^{(2)}$. We have

$$\mathcal{L}_{II}^{(2)} = -\frac{4v}{f^2}\mathrm{Tr}\left(m_q M^2\right) + \cdots, \tag{2.30}$$

from which, we can read off

$$m_\pi^2 = \frac{8v}{f^2}\hat{m} \; ; \; m_K^2 = \frac{4v}{f^2}(\hat{m} + m_s) \; ; \; m_\eta^2 = \frac{8v}{3f^2}(\hat{m} + 2m_s), \tag{2.31}$$

where corrections of order $m_u - m_d$ have been ignored, and $\hat{m} = m_u = m_d$, in this approximation. From the expressions in (2.31), we can derive the following relation among the meson masses

$$3m_\eta^2 = 4m_K^2 - m_\pi^2, \tag{2.32}$$

which is known as the Gell-Mann-Okubo relation [14], derived here, using the chiral Lagrangian formalism.

Using the Noether procedure, one can derive the chiral current $J^{A\mu}$ representing the matrix element of a quark current in a flavor changing process. The current $J^{A\mu}$, at leading order in chiral perturbation theory, is given by

$$J^{A\mu} = -i\frac{f^2}{2}\mathrm{Tr}\left(T^A \Sigma\, \partial^\mu \Sigma^\dagger\right), \tag{2.33}$$

where $T^A$ is the appropriate matrix for a certain flavor changing process. For example, in the process $\pi^- \to \mu\, \bar{\nu}_\mu$, the matrix element for the quark current $\langle 0|\bar{u}\gamma_\mu(1-\gamma_5)d|\pi^-\rangle$ is given by

$$J^{A\mu} = -i\frac{f^2}{2}\mathrm{Tr}\left(T^A \Sigma\, \partial^\mu \Sigma^\dagger\right) = -f\partial^\mu \pi^- = i f p_\pi^\mu, \tag{2.34}$$

where $(T^A)_{ij} = \delta_{i1}\delta_{j2}$, and $p_\pi^\mu$ is the pion momentum. Since, by definition, $\langle 0|\bar{u}\gamma_\mu(1-\gamma_5)d|\pi^-\rangle = i f_\pi p_\mu$, we see that at leading order, $\mathcal{O}(p^2)$, in chiral perturbation theory, $f = f_\pi \approx 132$ MeV, where $f_\pi$ is the pion decay constant. Note that under $SU(3)_V$, at the leading order, $f_\pi = f_K = f_\eta$, and experimentally, $f_K \approx 1.2 f_\pi$, and $f_\eta \approx f_\pi$ [32], as a result of $\pi - \eta$ mixing.

This completes our description of the effective theory at $\mathcal{O}(p^2)$. One can systematically add terms of higher order in the derivative expansion to the Lagrangian

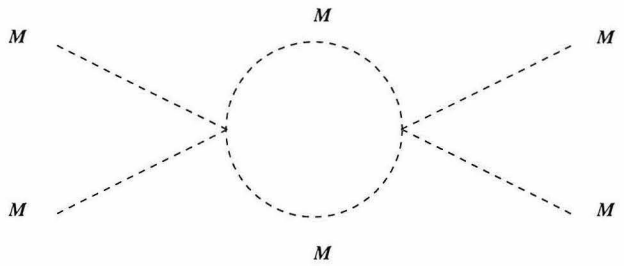


Figure 2.2: The Feynman diagram for the process $MM \to MM$ at 1-loop. The vertices are $\mathcal{O}(p^2)$ and the diagram contributes at $\mathcal{O}(p^4)$ in chiral perturbation theory.

(2.29). In loop calculations using chiral perturbation theory, each loop counts as an extra $p^2$ in the expansion. For example, using the $\mathcal{O}(p^2)$ vertex operators, a 1-loop calculation requires the inclusion of tree level $\mathcal{O}(p^4)$ terms which act as the counter terms in the renormalization of the loop diagrams. In this way, we end up with a well-defined systematic procedure for calculating various diagrams describing low energy hadronic interactions. However, the coefficients of the higher order terms have to be phenomenologically fixed.

Before closing this chapter, we include a heuristic estimate presented in Ref. [23] for the size of chiral symmetry breaking scale $\Lambda_{\chi B}$, which is the momentum scale at which chiral perturbation expansion becomes unreliable. To do this, we examine the amplitude for the scattering $MM \to MM$, where $M$ denotes one of the eight pseudoscalar fields, at 1-loop, using the $\mathcal{O}(p^2)$ vertices of the chiral Lagrangian (2.26). In Fig. (2.2), we present the Feynman diagram for this scattering. Each $\mathcal{O}(p^2)$ vertex $\mathcal{V}$ has the form

$$\mathcal{V} \sim \frac{p^2 M^4}{f^2}, \tag{2.35}$$

where $p$ is a typical momentum. The scattering amplitude receives a contribution from the term $\mathcal{A}$ in which the derivatives act on the external legs of the diagram in Fig. (2.2),

$$\mathcal{A} \sim \frac{p^4 M^4}{f^4} \int \frac{d^4k}{(2\pi)^4} \frac{1}{(k^2)^2}\,, \tag{2.36}$$

where $k$ is the momentum that runs in the loop. The loop integral can be regulated in the ultraviolet by a cutoff $\Lambda_{\chi B}$, the scale above which the effective chiral Lagrangian becomes unreliable. We then have

$$\mathcal{A} \sim \frac{p^4 M^4}{f^4} \frac{1}{(4\pi)^2} \ln\left(\frac{\Lambda_{\chi B}^2}{\mu^2}\right), \tag{2.37}$$

where $\mu$ is some arbitrary renormalization scale for the external momenta. The process $MM \to MM$ also receives a contribution of the form (2.37) from an $\mathcal{O}(p^4)$ term $\mathcal{L}^{(4)}$ given by

$$\mathcal{L}^{(4)} \sim \frac{f^2}{\Lambda_{\chi B}^2} \mathrm{Tr}\left(\partial_\mu \Sigma \, \partial_\nu \Sigma^\dagger \, \partial^\mu \Sigma \, \partial^\nu \Sigma^\dagger\right). \tag{2.38}$$

Changes in $\mu$ can be absorbed into the coefficient of $\mathcal{L}^{(4)}$, by a redefinition. Therefore, in the absence of an accidental fine-tuning of the parameters in the effective Lagrangian, we expect the coefficient of $\mathcal{L}^{(4)}$ to be at least as large as the coefficient induced by an $\mathcal{O}(1)$ rescaling of $\mu$ in Eq. (2.37). Thus, we may write

$$\frac{f^2}{\Lambda_{\chi B}^2} \gtrsim \frac{1}{(4\pi)^2} \Rightarrow \Lambda_{\chi B} \lesssim 4\pi f. \tag{2.39}$$

Since $f \sim 100$ MeV, (2.39) yields

$$\Lambda_{\chi B} \lesssim 1\,\mathrm{GeV}. \tag{2.40}$$

Therefore, we conclude that as long as we consider only processes in which all the components of the pseudo-Goldstone boson 4-momenta $p^\mu$ satisfy $p^\mu << 1$ GeV, chiral perturbation theory provides a controlled and systematic approach to calculating the low energy hadronic interactions involving the pseudo-Goldstone bosons.

In chapters 3, 4, and 5, we use the methods introduced in this chapter as the basis of our treatment of various phenomena. In order to do this, we need to augment the effective Lagrangian (2.29) with additional terms. However, chiral symmetry and expansion in powers of momenta, as introduced here, will be used as the basic

principles underlying all of the calculations that will follow.

# Chapter 3 Chiral Perturbation Theory for $\tau \to \rho\pi\nu_\tau$, $\tau \to K^*\pi\nu_\tau$, and $\tau \to \omega\pi\nu_\tau$

## 3.1 Introduction

Chiral perturbation theory has been applied to describe strong interactions of the lowest lying vector mesons $\rho, K^*, \omega$, and $\phi$ with the pseudo-Goldstone bosons [15]. The vector mesons can be treated as heavy and an effective Lagrangian based on the $SU(3)_L \times SU(3)_R$ chiral symmetry can be written down for couplings between the vector mesons and the pseudo-Goldstone bosons. At leading order in the derivative expansion, the chiral Lagrangian has two coupling constants $g_1$ and $g_2$ that are related in the large $N_c$ (i.e., number of colors) limit [16]. While it is known from the value of the octet-singlet mixing angle and the smallness of the $\phi \to \rho\pi$ amplitude that the $N_c \to \infty$ relation, $g_1 = 2g_2/\sqrt{3}$, is a reasonable approximation, the value of $g_2$ has not been determined.

In this chapter, we use heavy vector meson chiral perturbation theory to study the decays $\tau \to \rho\pi\nu_\tau$ and $\tau \to K^*\pi\nu_\tau$ in the kinematic regime where the pion is "soft" in the vector meson's rest frame. At the present time, there is little experimental information that bears on the applicability of chiral perturbation theory for vector meson interactions. These $\tau$ decays provide an interesting way to test whether low orders in the momentum expansion yield a good approximation. Using the large $N_c$ limit, we also predict the differential decay rate for $\tau \to \omega\pi\nu_\tau$, in the kinematic regime where the pion is soft in the $\omega$ rest frame. In heavy vector meson chiral perturbation theory, this decay amplitude is dominated by a $\rho$ pole and is proportional to $g_2^2$. Comparing with experimental data [17], we find that $|g_2| \approx 0.6$. An important aspect of this work is that we will only use chiral $SU(2)_L \times SU(2)_R$ symmetry and consequently do not treat the strange quark mass as small.

The decays $\tau \to \rho\pi\nu_\tau, \tau \to K^*\pi\nu_\tau$, and $\tau \to \omega\pi\nu_\tau$ result in final hadronic states that contain three and four pseudo-Goldstone bosons. The amplitude for the vector and axial currents to produce pseudo-Goldstone bosons is determined by ordinary chiral perturbation theory [18] but only in a limited kinematic region where their invariant mass is small compared with the chiral symmetry breaking scale. The situation is similar for heavy vector meson chiral perturbation theory. It partially constrains the multi pseudo-Goldstone boson amplitudes in a small (but different) part of the available phase space. This chapter is meant to illustrate the usefulness of heavy vector meson chiral perturbation theory for $\tau$ decay. Since the $\rho$ and $K^*$ widths are not negligible, a more complete calculation that includes vector meson decay and interference between different vector meson amplitudes that give the same three pseudo-Goldstone boson final hadronic state may be necessary for a detailed comparison with experiment in these cases.

For the $\tau$ decays $\tau \to \rho\nu_\tau, \tau \to K^*\nu_\tau, \tau \to \rho\pi\nu_\tau$, $\tau \to K^*\pi\nu_\tau$, and $\tau \to \omega\pi\nu_\tau$, we need matrix elements of the left-handed currents $\bar{d}\gamma_\mu(1-\gamma_5)u$ and $\bar{s}\gamma_\mu(1-\gamma_5)u$ between the vacuum and a vector meson or a vector meson and a low momentum pion. In the next section, we derive the hadron level operators that represent these currents in chiral perturbation theory. Section 3.3 contains expressions for the $\tau \to \rho\pi\nu_\tau$, $\tau \to K^*\pi\nu_\tau$, and $\tau \to \omega\pi\nu_\tau$ differential decay rates. A summary of the issues discussed in this chapter is presented in Section 3.4.

## 3.2 Chiral Perturbation Theory for Vector Mesons

An effective Lagrangian based on $SU(2)_L \times SU(2)_R$ chiral symmetry that describes the interactions of $\rho$ and $K^*$ vector mesons with pions can be derived in the standard way. The pions are incorporated into a $2 \times 2$ special unitary matrix

$$\Sigma = \exp(2i\Pi/f), \tag{3.1}$$

where

$$\Pi = \begin{bmatrix} \pi^0/\sqrt{2} & \pi^+ \\ \pi^- & -\pi^0/\sqrt{2} \end{bmatrix}. \tag{3.2}$$

Under chiral $SU(2)_L \times SU(2)_R, \Sigma \to L\Sigma R^\dagger$, where $L \in SU(2)_L$ and $R \in SU(2)_R$. As mentioned before, at leading order in chiral perturbation theory, $f$ can be identified with the pion decay constant $f_\pi \approx 132$ MeV. For describing the interactions of the pions with other fields it is convenient to introduce

$$\xi = \exp\left(\frac{i\Pi}{f}\right) = \sqrt{\Sigma}. \tag{3.3}$$

Under chiral $SU(2)_L \times SU(2)_R$,

$$\xi \to L\xi U^\dagger = U\xi R^\dagger, \tag{3.4}$$

where $U$ is a complicated function of $L, R$, and the pion fields $\Pi$. However, in the special case of transformations where $L = R = V$ in the unbroken $SU(2)_V$ vector subgroup, $U = V$.

The $\rho$ fields are introduced as a $2 \times 2$ matrix

$$R_\mu = \begin{bmatrix} \rho_\mu^0/\sqrt{2} & \rho_\mu^+ \\ \rho_\mu^- & -\rho_\mu^0/\sqrt{2} \end{bmatrix}, \tag{3.5}$$

and the $K^*, \bar{K}^*$ fields as doublets

$$K_\mu^* = \begin{bmatrix} K_\mu^{*+} \\ K_\mu^{*0} \end{bmatrix}, \qquad \bar{K}_\mu^* = \begin{bmatrix} K_\mu^{*-} \\ \bar{K}_\mu^{*0} \end{bmatrix}. \tag{3.6}$$

Under chiral $SU(2)_L \times SU(2)_R$,

$$R_\mu \to U R_\mu U^\dagger, \quad K_\mu^* \to U K_\mu^*, \ \bar{K}_\mu^* \to U^* \bar{K}_\mu^*. \tag{3.7}$$

The doublets $K_\mu^*$ and $\bar{K}_\mu^*$ are related by charge conjugation which acts on the fields as follows:

$$CR_\mu C^{-1} = -R_\mu^T, \quad CK_\mu^* C^{-1} = -\bar{K}_\mu^*, \quad C\xi C^{-1} = \xi^T. \tag{3.8}$$

We construct an effective Lagrangian for strong transitions of the form $V \to V'X$, where $V$ and $V'$ are vector mesons and $X$ is either the vacuum or one or more soft pions. The vector meson fields are treated as heavy with fixed four velocity $v^\mu, v^2 = 1$, satisfying the constraint $v \cdot R = v \cdot K^* = v \cdot \bar{K}^* = 0$. The chiral Lagrange density has the general structure

$$\mathcal{L} = \mathcal{L}_{kin} + \mathcal{L}_{int} + \mathcal{L}_{mass} - \frac{i}{2}\mathcal{L}_{width}. \tag{3.9}$$

The interaction terms are

$$\mathcal{L}_{int} = ig_2^{(\rho)}\mathrm{Tr}(\{R_\mu^\dagger, R_\nu\}A_\lambda)v_\sigma\epsilon^{\mu\nu\lambda\sigma} + ig_2^{(K^*)}\bar{K}_\mu^{*\dagger}A_\lambda^T\bar{K}_\nu^* v_\sigma\epsilon^{\mu\nu\lambda\sigma} + ig_2^{(K^*)}K_\mu^{*\dagger}A_\lambda K_\nu^* v_\sigma\epsilon^{\mu\nu\lambda\sigma}, \tag{3.10}$$

where

$$A_\lambda = \frac{i}{2}(\xi\partial_\lambda\xi^\dagger - \xi^\dagger\partial_\lambda\xi). \tag{3.11}$$

Comparing with the Lagrange density in Eq. (11) of Ref. [15], we find that in the case of $SU(3)_L \times SU(3)_R$ symmetry $g_2^{(\rho)} = g_2^{(K^*)} = g_2$, at leading order in $SU(3)_L \times SU(3)_R$ chiral perturbation theory. At higher orders, integrating out the kaons will lead to a difference between $g_2^{(\rho)}$ and $g_2^{(K^*)}$. Note that for the vector mesons $\rho_\mu^{-\dagger} \neq \rho_\mu^+$, etc. In heavy vector meson chiral perturbation theory, $\rho_\mu^+$ destroys a $\rho^+$, but it does not create the corresponding antiparticle. The field $\rho_\mu^{-\dagger}$ creates a $\rho^-$.

The kinetic terms are

$$\begin{aligned}\mathcal{L}_{kin} = & - i\mathrm{Tr}R_\mu^\dagger v\cdot\partial R^\mu - i\mathrm{Tr}R_\mu^\dagger[v\cdot V, R^\mu] - iK_\mu^{*\dagger}v\cdot\partial K^{*\mu} - iK_\mu^{*\dagger}v\cdot VK^{*\mu} \\ & - i\bar{K}_\mu^{*\dagger}v\cdot\partial\bar{K}^{*\mu} + i\bar{K}_\mu^{*\dagger}v\cdot V^T\bar{K}^{*\mu}, \end{aligned} \tag{3.12}$$

where

$$V_\nu = \frac{1}{2}(\xi\partial_\nu\xi^\dagger + \xi^\dagger\partial_\nu\xi). \tag{3.13}$$

The mass terms are

$$\begin{aligned}\mathcal{L}_{mass} = & \lambda_2^{(\rho)}\mathrm{Tr}(\{R_\mu^\dagger, R^\mu\}M_\xi) + \lambda_2^{(K^*)}K_\mu^{*\dagger}M_\xi K^\mu + \lambda_2^{(K^*)}\bar{K}_\mu^{*\dagger}M_\xi^T\bar{K}^{*\mu} \\ & + \sigma_8^{(\rho)}\mathrm{Tr}(M_\xi)\mathrm{Tr}(R_\mu^\dagger R^\mu) + \sigma_8^{(K^*)}\mathrm{Tr}(M_\xi)K_\mu^{*\dagger}K^\mu \\ & + \sigma_8^{(K^*)}\mathrm{Tr}(M_\xi)\bar{K}_\mu^{*\dagger}\bar{K}^{*\mu}. \end{aligned} \tag{3.14}$$

In Eq. (3.14)

$$M_\xi = \frac{1}{2}(\xi M\xi + \xi^\dagger M\xi^\dagger), \tag{3.15}$$

where

$$M = \begin{bmatrix} m_u & 0 \\ 0 & m_d \end{bmatrix} \tag{3.16}$$

is the quark mass matrix. At leading order in $SU(3)_L \times SU(3)_R$ chiral perturbation theory, the couplings in Eq. (3.14) are related to those in Ref. [15] by

$$\lambda_2^{(\rho)} = \lambda_2^{(K^*)} = \lambda_2 \text{ and } \sigma_8^{(\rho)} = \sigma_8^{(K^*)} = \sigma_8. \tag{3.17}$$

The $\rho$ and $K^*$ are not stable. In heavy vector meson chiral perturbation theory, their widths appear as antihermitian terms in the Lagrange density (3.9). Since the $\rho$ and $K^*$ widths vanish in the large $N_c$ (i.e., number of colors) limit and are comparable

with the pion mass, we treat the widths as of order one derivative (the mass terms in (3.14) go like two derivatives and are less important in chiral perturbation theory than the terms in $\mathcal{L}_{kin}, \mathcal{L}_{int}$ and $\mathcal{L}_{width}$). The width terms are

$$\mathcal{L}_{width} = \Gamma^{(\rho)} \mathrm{Tr} R_\mu^\dagger R^\mu + \Gamma^{(K^*)} K_\mu^{*\dagger} K^{*\mu} + \Gamma^{(K^*)} \bar{K}_\mu^{*\dagger} \bar{K}^{*\mu}. \tag{3.18}$$

In the $SU(3)$ limit $\Gamma^{(\rho)} = \Gamma^{(K^*)}$, however, the physical values of the widths $\Gamma^{(\rho)} = 151$ MeV and $\Gamma^{(K^*)} = 50$ MeV are far from this situation. In heavy vector meson chiral perturbation theory, the vector meson propagator is

$$\frac{-i(g^{\mu\nu} - v^\mu v^\nu)}{v \cdot k + i\Gamma/2}, \tag{3.19}$$

where $\Gamma$ is the corresponding width. Note that we are treating the vector meson widths differently than Ref. [15]. In Ref. [15], chiral $SU(3)_L \times SU(3)_R$ was used and since the vector meson widths are small compared with the kaon mass they were treated as of the order of a light quark mass or, equivalently, two derivatives. Hence, in Ref. [15], the widths could be neglected in the propagator at leading order in chiral perturbation theory.

At the quark level, the effective Hamiltonian density for weak semileptonic $\tau$ decay is

$$\mathcal{H}_W = \frac{G_F}{\sqrt{2}} V_{ud} \bar{\nu}_\tau \gamma_\mu (1 - \gamma_5) \tau \bar{d} \gamma^\mu (1 - \gamma_5) u + \frac{G_F}{\sqrt{2}} V_{us} \bar{\nu}_\tau \gamma_\mu (1 - \gamma_5) \tau \bar{s} \gamma^\mu (1 - \gamma_5) u, \tag{3.20}$$

where $G_F$ is the Fermi constant and $V_{ud}$ and $V_{us}$ are elements of the Cabibbo-Kobayashi-Maskawa matrix where, experimentally, $|V_{ud}| \approx 1$ and $|V_{us}| \approx 0.22$. At leading order in chiral perturbation theory, we need to represent the currents $\bar{d}\gamma^\mu(1 - \gamma_5)u$ and $\bar{s}\gamma^\mu(1-\gamma_5)u$ by operators involving the hadron fields that transform respectively as $(3_L, 1_R)$ and $(2_L, 1_R)$ under chiral $SU(2)_L \times SU(2)_R$ and contain the least number of derivatives or insertions of the light quark mass matrix. These operators

are

$$\bar{d}\gamma_\mu(1-\gamma_5)u = \frac{f_\rho}{\sqrt{2m_\rho}}\mathrm{Tr}R_\mu^\dagger\xi^\dagger\begin{pmatrix}0&0\\1&0\end{pmatrix}\xi, \tag{3.21}$$

and

$$\bar{s}\gamma_\mu(1-\gamma_5)u = \frac{f_{K^*}}{\sqrt{2m_{K^*}}}\bar{K}_\mu^{*\dagger}\xi^T\begin{pmatrix}1\\0\end{pmatrix}. \tag{3.22}$$

The coefficients are fixed in terms of the vector meson decay constants $f_\rho$ and $f_{K^*}$ by the matrix elements $< K^{*-}|\bar{s}\gamma_\mu(1-\gamma_5)u|0 >$ and $< \rho^-|\bar{d}\gamma_\mu(1-\gamma_5)u|0 >$, which are equal to $f_{K^*}\epsilon_\mu^*$ and $f_\rho\epsilon_\mu^*$ respectively, and follow from Eqs. (3.21) and (3.22) by setting $\xi$ equal to unity. (Note that because of the parity invariance of the strong interactions the axial currents do not contribute to these matrix elements.)

In the large $N_c$ limit, couplings involving the $\omega$ are related to those involving the $\rho$. They can be derived from the Lagrange densities in Eqs. (3.10), (3.12), (3.14), and the expression for the current in Eq. (3.21) by replacing the isospin triplet matrix $R_\mu$ by the quartet matrix

$$Q_\mu = \begin{bmatrix}\rho_\mu^0/\sqrt{2}+\omega_\mu/\sqrt{2} & \rho_\mu^+\\ \rho_\mu^- & -\rho_\mu^0/\sqrt{2}+\omega_\mu/\sqrt{2}\end{bmatrix}. \tag{3.23}$$

However, the effect of the $\omega$ width cannot be included by replacing $R_\mu$ in Eq. (3.18) with $Q_\mu$. Since the widths vanish in the large $N_c$ limit, a separate term $\Gamma^{(\omega)}\omega_\mu^\dagger\omega^\mu$ must be added to Eq. (3.18). Experimentally, $\Gamma^{(\omega)} = 8.4$ MeV.

## 3.3 Differential Decay Rates

The amplitude for $\tau \to \rho\pi\nu_\tau$ follows from the Feynman diagram for the vacuum to $\rho\pi$ matrix element of the current shown in Fig. (3.1). Note that there is no pole diagram since the Lagrange density (3.10) has no $\rho\rho\pi$ coupling. The invariant matrix

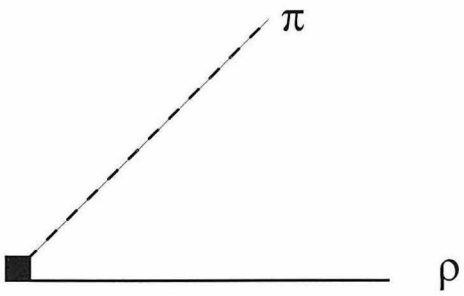


Figure 3.1: Feynman diagram representing the matrix element of the left-handed current from the vacuum to $\rho\pi$. In this case, only the axial current contributes.

element is

$$\mathcal{M}(\tau \to \rho^0 \pi^- \nu_\tau) = \frac{G_F V_{ud} f_\rho}{f_\pi} \bar{u}_\nu \gamma^\mu \epsilon^*_\mu(\rho)(1-\gamma_5) u_\tau, \tag{3.24}$$

where $u_{\nu,\tau}$ are four component spinors for the neutrino and the $\tau$.

It is convenient to express the differential decay distribution in terms of the $\rho\pi$ mass $s = (p_\rho + p_\pi)^2$ and the angle $\theta$ between the $\rho$ direction and the $\tau$ direction in the $\rho - \pi$ center of mass frame. Then the differential decay rate is

$$\frac{d\Gamma(\tau \to \rho^0 \pi^- \nu_\tau)}{ds d\cos\theta} = \frac{G_F^2 |V_{ud}|^2 f_\rho^2 m_\tau}{2^7 f_\pi^2 \pi^3} \left(1 - \frac{s}{m_\tau^2}\right) \sqrt{\frac{(s - m_\rho^2 + m_\pi^2)^2 - 4m_\pi^2 s}{4s^2}}$$

$$\times [A(s) + B(s)\cos\theta + C(s)\cos^2\theta], \tag{3.25}$$

where the dimensionless functions $A(s), B(s)$ and $C(s)$ are

$$A(s) = \frac{1}{8s^2 m_\rho^2} \left(1 - \frac{s}{m_\tau^2}\right) [(s + m_\rho^2 - m_\pi^2)^2 (s + m_\tau^2) + 4s^2 m_\rho^2], \tag{3.26}$$

$$B(s) = -\frac{m_\tau^2}{4s^2 m_\rho^2} \left(1 - \frac{s}{m_\tau^2}\right) (s + m_\rho^2 - m_\pi^2) \sqrt{(s - m_\rho^2 + m_\pi^2)^2 - 4m_\pi^2 s}, \tag{3.27}$$

and

$$C(s) = \frac{m_\tau^2}{8s^2 m_\rho^2}\left(1 - \frac{s}{m_\tau^2}\right)^2 [(s - m_\rho^2 + m_\pi^2)^2 - 4m_\pi^2 s]. \tag{3.28}$$

The differential decay rate is the same for the $\rho^-\pi^0$ mode. Our expression for the invariant matrix element in Eq. (3.24) was derived using heavy vector meson chiral perturbation theory, which is an expansion in $m_\pi/m_\rho$ and $v \cdot p_\pi/m_\rho$. In $A$, $B$, and $C$, terms suppressed by powers of these quantities should be neglected. To focus on the kinematic region where chiral perturbation theory is valid, it is convenient to change from the variable $s$ to the dimensionless variable $x = v \cdot p_\pi/m_\pi$, using

$$s = m_\rho^2 + m_\pi^2 + 2m_\pi m_\rho x. \tag{3.29}$$

Then expanding in $(m_\pi/m_\rho)$,

$$A(x) \approx \frac{1}{2}\left(1 - \frac{m_\rho^2}{m_\tau^2}\right)\left[2 + \frac{m_\tau^2}{m_\rho^2}\right], \tag{3.30}$$

$$B(x) \approx -\left(\frac{m_\pi}{m_\rho}\right)\left(\frac{m_\tau^2}{m_\rho^2} - 1\right)\sqrt{x^2 - 1}, \tag{3.31}$$

and

$$C(x) \approx \frac{1}{2}\left(\frac{m_\pi^2}{m_\rho^2}\right)\left(\frac{m_\tau^2}{m_\rho^2}\right)\left(1 - \frac{m_\rho^2}{m_\tau^2}\right)^2 (x^2 - 1). \tag{3.32}$$

Hence, $B$ and $C$ are negligible compared with $A$ and our expression for the differential decay rate becomes

$$\frac{d\Gamma(\tau \to \rho^0\pi^-\nu_\tau)}{dx\, d\cos\theta} = \frac{G_F^2 |V_{ud}|^2 f_\rho^2 m_\tau m_\pi^2}{2^7 f_\pi^2 \pi^3}\sqrt{x^2 - 1}\left(1 - \frac{m_\rho^2}{m_\tau^2}\right)^2\left[2 + \frac{m_\tau^2}{m_\rho^2}\right]. \tag{3.33}$$

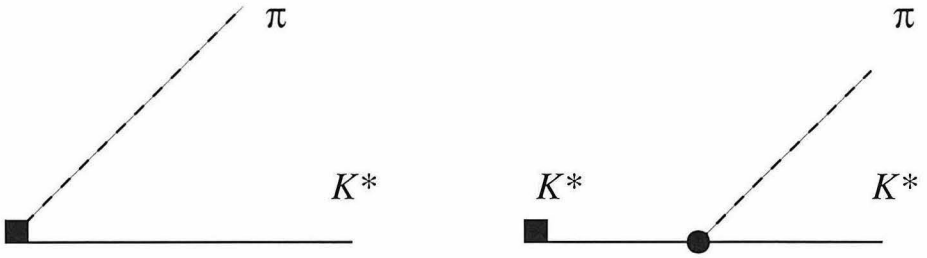


Figure 3.2: Feynman diagrams representing the matrix element of the left-handed current from the vacuum to $K^*\pi$. For the first diagram, the axial current contributes while for the second pole diagram, the vector current contributes.

Normalizing to the $\tau \to \rho^- \nu_\tau$ width gives the simple expression

$$\frac{1}{\Gamma(\tau \to \rho^- \nu_\tau)} \frac{d\Gamma(\tau \to \rho^0 \pi^- \nu_\tau)}{dx} = \left(\frac{m_\pi}{f_\pi}\right)^2 \frac{\sqrt{x^2-1}}{4\pi^2}. \tag{3.34}$$

It seems reasonable that lowest order chiral perturbation theory will be a useful approximation in the region $x \in [1,2]$. Integrating $x$ over this region gives a $\tau \to \rho^0 \pi^- \nu_\tau$ width that is 0.03 times the $\tau \to \rho^- \nu_\tau$ width.

The amplitude for $\tau \to K^* \pi \nu_\tau$ follows from the Feynman diagrams for the vacuum to $K^*\pi$ matrix element of the left-handed current shown in Fig. (3.2). In this case, there is a pole contribution proportional to the $K^*K^*\pi$ coupling $g_2^{(K^*)}$. The resulting invariant matrix element is

$$\mathcal{M}(\tau \to \bar{K}^{*0} \pi^- \nu_\tau) = \frac{G_F V_{us} f_{K^*}}{\sqrt{2} f_\pi} \bar{u}_\nu \gamma_\mu (1-\gamma_5) u_\tau$$

$$\times \left[ \epsilon^{*\mu}(K^*) + \frac{i g_2^{(K^*)} \epsilon^{\nu\mu\beta\sigma}}{(v \cdot p_\pi + i\Gamma^{(K^*)}/2)} p_{\pi\beta} v_\sigma \epsilon^*_\nu(K^*) \right]. \tag{3.35}$$

The term proportional to $g_2^{(K^*)}$ arises from the pole diagram and it corresponds to the $p$-wave $K^*\pi$ amplitude. In the non-relativistic constituent quark model [19] $g_2^{(K^*)} = 1$. Following the same procedure as for the $\tau \to \rho\pi\nu_\tau$ case, we arrive at the

differential decay rate

$$\frac{d\Gamma(\tau \to \bar{K}^{*0}\pi^-\nu_\tau)}{dx d\cos\theta} = \frac{G_F^2 |V_{us}|^2 f_{K^*}^2 m_\pi^2 m_\tau}{2^8 f_\pi^2 \pi^3} \sqrt{x^2-1}\left(1-\frac{m_{K^*}^2}{m_\tau^2}\right)^2$$

$$\times \left\{ \left(\frac{m_\tau^2}{m_{K^*}^2}+2\right) + \frac{g_2^{(K^*)2}}{x^2(1+\gamma^2)}\left(\frac{m_\tau^2}{m_{K^*}^2}+1\right)(x^2-1) \right.$$

$$\left. + \frac{4g_2^{(K^*)}}{x(1+\gamma^2)}\sqrt{x^2-1}\cos\theta - \frac{g_2^{(K^*)^2}}{x^2(1+\gamma^2)}(x^2-1)\left(\frac{m_\tau^2}{m_{K^*}^2}-1\right)\cos^2\theta \right\}. \tag{3.36}$$

In Eq. (3.36),

$$\gamma = \Gamma^{(K^*)}/(2x m_\pi). \tag{3.37}$$

In this case, $s = m_{K^*}^2 + m_\pi^2 + 2m_\pi m_{K^*} x$. The rate for $\tau \to K^{*-}\pi^0\nu_\tau$ is one half the rate for $\tau \to \bar{K}^{*0}\pi^-\nu_\tau$.

Normalizing to the $\tau \to K^{*-}\nu_\tau$ decay width and integrating over $x \in$ [1,2], Eq. (3.36) gives

$$\frac{1}{\Gamma(\tau \to K^{*-}\nu_\tau)} \int_1^2 dx \frac{d\Gamma(\tau \to \bar{K}^{*0}\pi^-\nu_\tau)}{dx d\cos\theta} \approx 7.5 \times 10^{-3}[(1 + 0.48 g_2^{(K^*)^2})$$

$$+0.51 g_2^{(K^*)}\cos\theta - 0.28 g_2^{(K^*)^2}\cos^2\theta]. \tag{3.38}$$

The shape of the $\bar{K}^{*0}\pi^-\nu_\tau$ decay distribution in $\cos\theta$ depends on the value of $g_2^{(K^*)}$ and it may be possible at a $\tau$-charm or $B$ factory to determine this coupling from a study of $\tau \to K^*\pi\nu_\tau$ decay. In the $SU(3)$ limit $g_2^{(K^*)} = g_2^{(\rho)}$ and in what follows we discuss how to determine $g_2^{(\rho)}$ in the large $N_c$ limit.

Using both heavy vector meson chiral perturbation theory and the large $N_c$ limit, the amplitude for $\tau \to \omega\pi\nu_\tau$ follows from the Feynman diagram for vacuum to $\omega\pi$ matrix element of the left-handed current in Fig. (3.3). In this case, there is only a

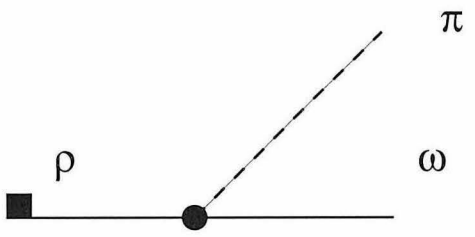


Figure 3.3: Feynman diagram representing the matrix element of the left-handed current from the vacuum to $\omega\pi$. In this case, only the vector current contributes.

pole graph and the invariant matrix element is

$$\mathcal{M}(\tau \to \omega\pi^-\nu_\tau) = \frac{G_F V_{ud} f_\rho}{f_\pi} \bar{u}_\nu \gamma_\mu (1-\gamma_5) u_\tau \left[ \frac{i g_2^{(\rho)}}{(v\cdot p_\pi + i\Gamma^{(\rho)}/2)} \quad \epsilon^{\nu\mu\beta\sigma} p_{\pi\beta} v_\sigma \epsilon^*_\nu(\omega) \right]. \tag{3.39}$$

Here, the difference between the $\rho$ and $\omega$ masses is neglected as is appropriate in the large $N_c$ limit. The resulting differential decay rate is

$$\frac{d\Gamma(\tau \to \omega\pi^-\nu_\tau)}{dx\, d\cos\theta} = \frac{G_F^2 |V_{ud}|^2 f_\rho^2 m_\pi^2 m_\tau}{2^7 f_\pi^2 \pi^3} (x^2-1)^{3/2} \left(1 - \frac{m_\omega^2}{m_\tau^2}\right)^2$$

$$\times \frac{g_2^{(\rho)^2}}{x^2(1+\gamma^2)} \left[ \left( \frac{m_\tau^2}{m_\omega^2} + 1 \right) - \left( \frac{m_\tau^2}{m_\omega^2} - 1 \right) \cos^2\theta \right], \tag{3.40}$$

where now

$$\gamma = \Gamma^{(\rho)}/(2x m_\pi), \tag{3.41}$$

and $s = m_\omega^2 + m_\pi^2 + 2 m_\omega m_\pi x$. Integrating over $\cos\theta$ and dividing by the rate for $\tau \to \rho\nu_\tau$ give (again we neglect the difference between the $\rho$ and $\omega$ masses) the simple expression,

$$\frac{1}{\Gamma(\tau \to \rho^-\nu_\tau)} \frac{d\Gamma(\tau \to \omega\pi^-\nu_\tau)}{dx} = \left( \frac{m_\pi}{f_\pi} \right)^2 \frac{(x^2-1)^{3/2} g_2^{(\rho)^2}}{6\pi^2 x^2 (1+\gamma^2)}. \tag{3.42}$$

Ref. [17] plots the differential decay rate as a function of the $\omega\pi$ invariant mass [see

Fig. 3(b)]. The first bin corresponds to $x \leq 1.7$. Integrating the $\tau \to \omega\pi\nu_\tau$ differential decay rate over $x \in [1, 1.7]$ and comparing with the experimental rate in this region [20] give $|g_2^{(\rho)}| \approx 0.57$. If both the first and second bins are included, the region corresponds to $x \in [1, 2.7]$ and integrating over this region gives $|g_2^{(\rho)}| \approx 0.65$. It is not likely that lowest order chiral perturbation theory will be a good approximation for values of $x$ greater than this.

## 3.4 Summary and Remarks

In this chapter, we have studied the decay modes $\tau \to \rho\pi\nu_\tau$, $\tau \to K^*\pi\nu_\tau$, and $\tau \to \omega\pi\nu_\tau$, using heavy vector meson chiral perturbation theory. Eqs. (3.33), (3.36), and (3.40) are our main results. Our predictions are valid in the kinematic region where the pion is soft in the vector meson rest frame. For these modes, vector meson decay results in three or four pseudo-Goldstone boson hadronic final states, and heavy vector meson chiral perturbation theory restricts these amplitudes in a small part of phase space. This is similar to applications of ordinary chiral perturbation theory which are valid in a different small kinematic region.

Modes similar to those discussed in this chapter, such as $\tau \to \rho K \nu_\tau$, can also be studied, using chiral perturbation theory. They will be related to those we considered in chiral $SU(3)_L \times SU(3)_R$. Using chiral $SU(3)_L \times SU(3)_R$, the left-handed current

$$J^A_{L\lambda} = \bar{q} T^A \gamma_\lambda (1 - \gamma_5) q \tag{3.43}$$

is represented by

$$J^A_{L\lambda} = \frac{f_V}{\sqrt{2 m_V}} \mathrm{Tr}(O^\dagger_\lambda \xi^\dagger T^A \xi), \tag{3.44}$$

where $O_\lambda$ is the $3 \times 3$ octet matrix of vector meson fields.

We found a branching ratio for $\tau \to \rho^0 \pi^- \nu_\tau$ in the region where the hadronic mass satisfies $m_{\rho\pi} < 1022$ MeV, of 0.69%, and a branching ratio for $\tau \to \bar{K}^{*0}\pi^-\nu_\tau$ in the region $m_{K^*\pi} < 1151$ MeV, of $(0.02 + 0.008 g_2^{(K^*)^2})\%$. It may be possible to study

$\tau \to K^*\pi\nu_\tau$ decay in the kinematic region where chiral perturbation theory is valid at a $\tau$-charm or $B$ factory [21].

In $\tau$ decay, the $\rho\pi$ final hadronic states get a significant contribution from the $a_1(1260)$ resonance which has a large width of around 400 MeV, while $K^*\pi$ final states get contributions from the $K_1(1270)$, $K_1(1400)$, and $K^*(1410)$ which have widths of 90 MeV, 174 MeV, and 227 MeV, respectively. Since in our formulation of chiral perturbation theory these heavier resonances are integrated out, one can take the view that the "tails" of their contributions are constrained by our results. Note that the $K_1(1270)$ has a branching ratio of only 16% to $K^*\pi$.

The narrow width of the $\omega$ makes $\tau \to \omega\pi\nu_\tau$ easier to study experimentally than $\tau \to \rho\pi\nu_\tau$. Using both heavy vector meson chiral perturbation theory and the large $N_c$ limit, we predicted the differential decay rate for $\tau \to \omega\pi\nu_\tau$ in the kinematic region where the pion is soft in the $\omega$ rest frame. Comparing with experimental data, we find that the $\rho\omega\pi$ coupling, $|g_2^{(\rho)}| \approx 0.6$. $\tau \to \omega\pi\nu_\tau$ decay proceeds via the vector part of the weak current and the rate for this decay is related by isospin to the $e^+e^- \to \omega\pi^0$ cross section. Experimental data [22] on $e^+e^- \to \omega\pi^0$ lead to a comparable value for $g_2^{(\rho)}$.

Our predictions for $\tau$ decay amplitudes get corrections suppressed by just $\sim v \cdot p_\pi/(1\text{GeV})$ from operators with one derivative (e.g., $\text{Tr}O_\lambda^\dagger v\cdot A\xi^\dagger T^A\xi$) that occur in the left-handed current. This is different from pseudo-Goldstone boson self interactions where corrections to leading order results are suppressed by $p^2/(1\text{GeV}^2)$, where $p$ is a typical momentum. Hence, even in the region, $1 < v \cdot p_\pi/m_\pi < 2$, we expect sizeable corrections to our results. This is particularly true for the $\rho\pi$ case where this region overlaps with a significant part of the $a_1$ Breit–Wigner distribution.

We have applied heavy vector meson chiral perturbation theory to $\tau$ decay and used data on $\tau \to \omega\pi\nu_\tau$ to determine the magnitude of the coupling $g_2$ in the chiral Lagrangian. The value we extract, $|g_2| \approx 0.6$, is not too far from the prediction, $g_2 = 0.75$, of the chiral quark model [23]. The value of $g_2$ is relevant for other processes of experimental interest. For example, heavy vector meson chiral perturbation theory can be used to predict differential decay rates for $D \to K^*\pi e^+\nu_e$ in the kinematic

region where both $p_D \cdot p_\pi / m_D$ and $p_{K^*} \cdot p_\pi / m_{K^*}$ are small compared with the chiral symmetry breaking scale. In this case, one combines chiral perturbation theory for hadrons containing a heavy quark [7] with heavy vector meson chiral perturbation theory. In the next chapter, we show how to do this.

# Chapter 4 The Decay $D^0 \to \bar{K}^{*0}\pi^- e^+ \nu_e$ in the Context of Chiral Perturbation Theory

## 4.1 Introduction

As mentioned in chapter 3, chiral perturbation theory, based on $SU(3)_L \times SU(3)_R$ chiral symmetry, has been applied to the interactions of pseudo-Goldstone bosons with the lowest lying vector mesons, $\rho$'s, $K^*$'s, $\omega$, and $\phi$ [15]. In the previous chapter, we made use of this approach in studying the decay of the $\tau$ in the channels $\tau \to \rho\pi\nu_\tau$, $\tau \to K^*\pi\nu_\tau$, and $\tau \to \omega\pi\nu_\tau$. This last decay mode was used to extract the absolute value of the $K^*K^*\pi$ coupling constant $\left|g_2^{(K^*)}\right|$, in the $SU(3)$ limit, from experimental data [24]. The decay rates in the above modes were calculated, using $SU(2)_L \times SU(2)_R$ chiral symmetry only, thus not treating the strange quark mass as small.

In this chapter, we use chiral perturbation theory for heavy charmed mesons [26] and heavy vector mesons [15], in the limit of $SU(2)_L \times SU(2)_R$ chiral symmetry, to calculate the differential decay rate for $D^0 \to \bar{K}^{*0}\pi^- e^+ \nu_e$ in a region of phase space where the pion is "soft" in the rest frames of both the $D^0$ and the $K^{*0}$. Currently, there is an upper bound of 1.3% on the branching ratio for this decay mode. To calculate the leading order amplitude, we need the matrix element of the left-handed current $\bar{s}\gamma_\mu(1-\gamma_5)c$, between a $D^*$ and a $K^*$. Since the form factors for this current are not measured, we relate them to the form factors of the same left-handed current between a $D$ and a $K^*$, using heavy quark symmetry [27, 28]. At the present time, one of the form factors of the $D \to K^*$ current is still unmeasured. The dependence of the decay amplitude on this form factor is eliminated, since we study the decay in the region where the $K^*$ is near zero recoil. In this restricted region, the calculated

differential decay rate depends on the $DD^*\pi$ coupling constant $g_D$ of heavy charmed meson chiral perturbation Lagrangian (coupling constant $g$ of Eq. (12) in Ref. [26]). There is an experimental bound on the value of $g_D$, from $D^{*+} \to D^0\pi^+$, but the value of this constant remains to be measured directly. There have been theoretical attempts at the determination of $g_D$, such as those involving radiative $D^*$ decays [29, 30]. The recent work of Ref. [31] gives an extraction at 1-loop, using this method. Here, we present an independent theoretical approach for obtaining the value of $g_D$. The results of this chapter can be compared to the data on $D^0 \to \bar{K}^{*0}\pi^- e^+\nu_e$ to extract the experimental value of $g_D$ which can in turn provide a measure of the validity of the methods used here, by calculating other processes that depend on $g_D$ and comparing with data.

We will introduce the chiral perturbation theory relevant to this work, in the next section. In Section 4.3, we present expressions for the left-handed hadronic currents for $D \to K^*$ and $D^* \to K^*$, and the leading amplitude for the decay. Section 4.4 contains the prediction for the differential decay rate, in a restricted region of phase space that will be discussed. The concluding remarks are presented in Section 4.5, followed by an appendix in which some useful formulas are presented.

## 4.2 Chiral Perturbation Theory for $D^0 \to \bar{K}^{*0}\pi^- e^+\nu_e$

In this section, we introduce the formalism necessary for the calculations discussed in this chapter. In the rest of this chapter, the words "heavy meson" refer to a meson containing a charm or a bottom quark, unless otherwise specified. We will use notation similar to those of Refs. [26, 9]. We start with the strong interactions of pions and heavy mesons, under $SU(2)_L \times SU(2)_R$ chiral symmetry. As in the previous chapter, the pions are incorporated into a $2 \times 2$ special unitary matrix

$$\Sigma = \exp(2i\Pi/f_\pi), \tag{4.1}$$

where

$$\Pi = \begin{bmatrix} \pi^0/\sqrt{2} & \pi^+ \\ \pi^- & -\pi^0/\sqrt{2} \end{bmatrix}. \tag{4.2}$$

Under chiral $SU(2)_L \times SU(2)_R$, $\Sigma \to L\Sigma R^\dagger$, where $L \in SU(2)_L$ and $R \in SU(2)_R$. At the leading order in chiral perturbation theory, $f_\pi$ is given by the pion decay constant $f_\pi \approx 132$ MeV. To describe the interactions of pions with other fields, it is convenient to define

$$\xi \equiv \exp\left(\frac{i\Pi}{f_\pi}\right) = \sqrt{\Sigma}. \tag{4.3}$$

Under chiral $SU(2)_L \times SU(2)_R$,

$$\xi \to L\xi U^\dagger = U\xi R^\dagger, \tag{4.4}$$

where $U$ is a complicated function of $L, R$, and the pion fields $\Pi$. In the special case where $L = R = V$ in the unbroken $SU(2)_V$ vector subgroup, $U = V$.

We present an effective Lagrangian for the strong interactions of low momentum pions (in case of $SU(3)_L \times SU(3)_R$, these results will include kaons and the $\eta$, as well) with the ground state heavy mesons with $Q\bar{q}^a$ flavor quantum numbers, where $a = 1, 2$, and $q^1 = u$, $q^2 = d$. The light degrees of freedom have $s_l^{\pi_l} = \frac{1}{2}^-$ spin-parity quantum numbers, in these heavy mesons. In the limit where the mass of the heavy quark $m_Q \to \infty$, the spin of the light degrees of freedom combines with the spin of the heavy quark to yield two degenerate doublets, consisting of an $SU(2)_V$ antidoublet of pseudo-scalar mesons, denoted by $P_a$, and an $SU(2)_V$ antidoublet of vector mesons, denoted by $P_a^*$. We are interested in the case $Q = c$, for which the pseudo-scalar mesons are $D^0$ and $D^+$, and the vector mesons are $D^{*0}$ and $D^{*+}$. The above mentioned strong interaction Lagrangian, in addition to the usual symmetries, such as parity and Lorentz invariance, must have heavy quark symmetry, at the leading order. To proceed, it is convenient to incorporate the $P_a$ and $P_{a\mu}^*$ meson fields

into a $4 \times 4$ matrix $H_a$ [26, 25]

$$H_a = \frac{1+\not{v}}{2}(P^*_{a\mu}\gamma^\mu - P_a\gamma_5). \tag{4.5}$$

Note that the heavy fields $P_a$ and $P^*_{a\mu}$ only destroy their respective mesons of four-velocity $v$ and do not create the corresponding antiparticles. We have $v^\mu P^*_{a\mu} = 0$. Under $SU(2)_L \times SU(2)_R$

$$H_a \to H_b U^\dagger_{ba}, \tag{4.6}$$

where the repeated index $b$ is summed over 1 and 2, and $U$ was introduced in Eq. (4.4). Under the heavy quark spin symmetry group $SU(2)_v$, we have

$$H_a \to S H_a, \tag{4.7}$$

where $S \in SU(2)_v$. Lorentz transformations act on $H_a$ according to

$$H_a \to D(\Lambda) H_a D(\Lambda)^{-1}, \tag{4.8}$$

where $D(\Lambda)$ is an element of the $4 \times 4$ matrix representation of the Lorentz group.

We introduce

$$\bar{H}_a = \gamma^0 H^\dagger_a \gamma^0. \tag{4.9}$$

Thus, we get

$$\bar{H}_a = (P^{*\dagger}_{a\mu}\gamma^\mu + P^\dagger_a\gamma_5)\frac{1+\not{v}}{2}. \tag{4.10}$$

The transformation laws for $\bar{H}_a$ corresponding to those in Eqs. (4.6), (4.7), and (4.8), are

$$\bar{H}_a \to U_{ab}\bar{H}_b, \bar{H}_a \to \bar{H}_a S^{-1}, \text{ and } \bar{H}_a \to D(\Lambda)\bar{H}_a D(\Lambda)^{-1}. \tag{4.11}$$

The effective Lagrangian that describes the strong interactions of pions and heavy mesons, at leading order (one derivative), is then given by

$$\mathcal{L}^{(H)} = -i\mathrm{Tr}\bar{H}_a v\cdot\partial H_a + i\mathrm{Tr}\bar{H}_a H_b (v\cdot V)_{ba} - g_D \mathrm{Tr}\bar{H}_a H_b \gamma_\lambda\gamma_5 (A^\lambda)_{ba}, \tag{4.12}$$

where

$$V_\nu = \frac{1}{2}(\xi\partial_\nu\xi^\dagger + \xi^\dagger\partial_\nu\xi) \tag{4.13}$$

and

$$A_\lambda = \frac{i}{2}(\xi\partial_\lambda\xi^\dagger - \xi^\dagger\partial_\lambda\xi). \tag{4.14}$$

At the present time, there is only a bound on the coupling constant $g_D$ of Eq. (4.12), $g_D^2 < 0.45$, coming from the experimental bound $\Gamma(D^{*+} \to D^0\pi^+) < 0.09$ MeV [32]. The explicit chiral symmetry breaking terms contain light quark masses

$$\delta\mathcal{L}^{(1)} = \lambda_\xi \mathrm{Tr}\bar{H}_b H_a (M_\xi)_{ab} + \lambda_\Sigma \mathrm{Tr}\bar{H}_a H_a (M\Sigma + \Sigma^\dagger M)_{bb}. \tag{4.15}$$

In Eq. (4.15),

$$M_\xi = \frac{1}{2}(\xi M\xi + \xi^\dagger M\xi^\dagger), \tag{4.16}$$

where

$$M = \begin{bmatrix} m_u & 0 \\ 0 & m_d \end{bmatrix} \tag{4.17}$$

is the $2\times 2$ light quark mass matrix.

Eq. (4.12) yields the propagators $i\delta_{ab}/2v\cdot k$ and $-i\delta_{ab}(g^{\mu\nu} - v^\mu v^\nu)/2v\cdot k$ for $P_a$ and $P_a^*$, respectively, where $k$ is a small residual momentum. The leading heavy quark spin symmetry breaking effects at order $\Lambda_{QCD}/m_Q$, induced by the color-magnetic

operator [33], are given by

$$\delta\mathcal{L}^{(2)} = \frac{\lambda_Q}{m_Q}\mathrm{Tr}\bar{H}_a\sigma^{\mu\nu}H_a\sigma_{\mu\nu}. \tag{4.18}$$

In Eq. (4.15), $\lambda_\xi$ and $\lambda_\Sigma$ are dimensionless constants independent of the heavy quark mass, whereas $\lambda_Q$ of Eq. (4.18), with dimension 2, has a logarithmic dependence on the heavy quark mass [33], calculable in perturbative QCD. Under $SU(3)_L \times SU(3)_R$, the correspondence with the notation of Ref. [26] is given by

$$g_D = g, \lambda_\xi = 2\lambda_1, \lambda_\Sigma = \lambda_1', \text{ and } \lambda_Q = \lambda_2. \tag{4.19}$$

The only effect of the term in Eq. (4.18) is to change the $P_a$ and $P_a^*$ propagators, and an appropriate field redefinition [26] will yield $i\delta_{ab}/2v\cdot k$ and $-i\delta_{ab}(g^{\mu\nu}-v^\mu v^\nu)/2(v\cdot k-\Delta)$ for the aforementioned propagators, respectively, where

$$\Delta = m_{P^*} - m_P = \frac{-2\lambda_Q}{m_Q}. \tag{4.20}$$

Here, $Q = c$, and the mass difference $\Delta = m_{D^*} - m_D = 145$ MeV $\sim m_\pi$. Thus, $\Delta$ is considered as of order one derivative and has a leading order contribution in our subsequent calculations.

As in the previous chapter, the $K^*$ and $\bar{K}^*$ fields are introduced as doublets [9]

$$K_\mu^* = \begin{bmatrix} K_\mu^{*+} \\ K_\mu^{*0} \end{bmatrix}, \qquad \bar{K}_\mu^* = \begin{bmatrix} K_\mu^{*-} \\ \bar{K}_\mu^{*0} \end{bmatrix}. \tag{4.21}$$

Under chiral $SU(2)_L \times SU(2)_R$,

$$K_\mu^* \to UK_\mu^*, \ \bar{K}_\mu^* \to U^*\bar{K}_\mu^*. \tag{4.22}$$

The doublets $K_\mu^*$ and $\bar{K}_\mu^*$ are related by charge conjugation $C$ which acts on the fields

as follows:

$$CK_\mu^* C^{-1} = -\bar{K}_\mu^*, \quad C\xi C^{-1} = \xi^T. \tag{4.23}$$

The vector meson fields are treated as heavy with fixed four velocity $v'^\mu$, $v'^2 = 1$, satisfying the constraint $v' \cdot K^* = v' \cdot \bar{K}^* = 0$. Interactions of the form $V \to V'X$, where $V$ and $V'$ are $K^*$'s and $X$ is either the vacuum or one or more soft pions, are given by a Lagrangian of the form

$$\mathcal{L} = \mathcal{L}_{kin} + \mathcal{L}_{int} + \mathcal{L}_{mass} - \frac{i}{2}\mathcal{L}_{width}. \tag{4.24}$$

The interaction Lagrangian is given by

$$\mathcal{L}_{int} = ig_2^{(K^*)} \bar{K}_\mu^{*\dagger} A_\lambda^T \bar{K}_\nu^* v'_\sigma \epsilon^{\mu\nu\lambda\sigma} + ig_2^{(K^*)} K_\mu^{*\dagger} A_\lambda K_\nu^* v'_\sigma \epsilon^{\mu\nu\lambda\sigma}. \tag{4.25}$$

Here, $g_2^{(K^*)}$ in Eq. (4.25) and $g_2$ of the Lagrangian in Eq. (11) of Ref. [15] are equal, at the leading order in $SU(3)_L \times SU(3)_R$ chiral perturbation theory. Note that for the vector mesons $K_\mu^{-*\dagger} \neq K_\mu^{*+}$, and so on. In the heavy vector meson chiral perturbation theory, $K_\mu^{*+}$ destroys a $K^{*+}$, but it does not create its antiparticle $K^{-*}$. The field $K_\mu^{-*\dagger}$ creates a $K^{*-}$.

The kinetic terms in Lagrangian (4.24) are

$$\mathcal{L}_{kin} = -iK_\mu^{*\dagger} v' \cdot \partial K^{*\mu} - iK_\mu^{*\dagger} v' \cdot V K^{*\mu} - i\bar{K}_\mu^{*\dagger} v' \cdot \partial \bar{K}^{*\mu} + i\bar{K}_\mu^{*\dagger} v' \cdot V^T \bar{K}^{*\mu}. \tag{4.26}$$

The mass terms, which explicitly break chiral symmetry, are given by

$$\mathcal{L}_{mass} = \lambda_2^{(K^*)} K_\mu^{*\dagger} M_\xi K^{*\mu} + \lambda_2^{(K^*)} \bar{K}_\mu^{*\dagger} M_\xi^T \bar{K}^{*\mu} + \sigma_8^{(K^*)} \mathrm{Tr}(M_\xi) K_\mu^{*\dagger} K^{*\mu}$$

$$+\sigma_8^{(K^*)} \mathrm{Tr}(M_\xi) \bar{K}_\mu^{*\dagger} \bar{K}^{*\mu}. \tag{4.27}$$

At leading order in $SU(3)_L \times SU(3)_R$ chiral perturbation theory, the couplings in Eq. (4.27) are related to those of Ref. [15] by

$$\lambda_2^{(K^*)} = \lambda_2 \text{ and } \sigma_8^{(K^*)} = \sigma_8. \tag{4.28}$$

The $K^*$'s have a width $\Gamma^{(K^*)} = 50$ MeV. Since this width is comparable to the pion mass, we treat it as of order one derivative, and introduce it in our Lagrangian via the following terms

$$\mathcal{L}_{width} = \Gamma^{(K^*)} K_\mu^{*\dagger} K^{*\mu} + \Gamma^{(K^*)} \bar{K}_\mu^{*\dagger} \bar{K}^{*\mu}. \tag{4.29}$$

Note that the terms in Eqs. (4.25), (4.26), and (4.29) are of order one derivative and are considered of leading order, whereas the terms in Eq. (4.27) are proportional to light quark masses, which means they are of order two derivatives, and thus, considered non-leading in our calculations. In this formalism, the $K^*$ propagator is given by

$$\frac{-i(g^{\mu\nu} - v'^\mu v'^\nu)}{v' \cdot k' + i\Gamma^{(K^*)}/2}, \tag{4.30}$$

where $k'$ is the small residual momentum of the $K^*$.

## 4.3 Currents and the Amplitude

The part of the effective Hamiltonian $\mathcal{H}_W$ for weak semileptonic decay of $D^0$ that contributes to $D^0 \to \bar{K}^{*0}\pi^- e^+ \nu_e$, at the quark level, is given by

$$\mathcal{H}_W = \frac{G_F}{\sqrt{2}} V_{cs} \bar{\nu}_e \gamma_\mu (1 - \gamma_5) e^+ \bar{s} \gamma^\mu (1 - \gamma_5) c, \tag{4.31}$$

where $G_F$ is the Fermi constant, $V_{cs}$ is an element of the Cabibbo-Kobayashi-Maskawa matrix, and the spinors represent the corresponding fermions. Experimentally, we have $|V_{cs}| \approx 1$. The only Feynman diagrams that contribute at the leading order in

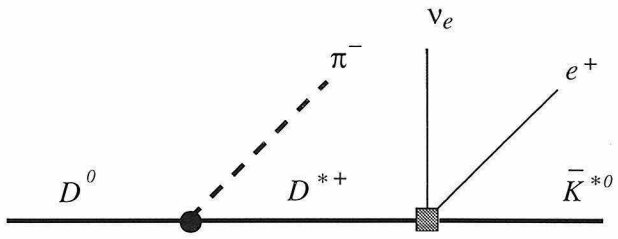


Figure 4.1: The $D^*$-pole diagram contribution to the amplitude in Eq. (4.41). The solid square represents the hadronic left-handed current and the solid circle represents the $DD^*\pi$ coupling proportional to $g_D$.

$SU(2)_L \times SU(2)_R$ chiral perturbation theory are presented in Figs. (4.1) and (4.2). We note that, of the non-leading diagrams, there are two that are not readily seen as higher order in our chiral perturbation expansion. One is the diagram with a direct $D^0\bar{K}^{*0}\pi^-$ current coupling to the leptonic current, or the non-pole diagram. The other diagram is the one in which the $K^{*-}$ in Fig. (4.2) has been replaced by a $K^-$, or the kaon-pole diagram.

To see why the non-pole diagram is subleading, we note that, under $SU(2)_L \times SU(2)_R$, the quark level current $\bar{s}\gamma^\mu(1-\gamma_5)c$ is a singlet, and thus the hadronic current which represents the quark level current must be a singlet as well. To make a singlet out of the $H, \bar{K}^*_\mu$, and $\xi$ fields, we need to have a $\partial^\mu\xi$ in the hadronic current expression. Thus, for the amplitude $A_1$ of the non-pole diagram we have $A_1 \propto p_\pi$. We have $p_\pi \sim m_\pi$, for a valid perturbative expansion, and thus $A_1 \to 0$, as $m_\pi \to 0$, in the chiral limit.

In the kaon-pole diagram, the $K^-\bar{K}^{*0}\pi^-$ coupling is proportional to $\partial^\mu\xi$, because only the pion has derivative coupling, being the only pseudo-Goldstone boson in the vertex. Hence, for the amplitude $A_2$ of this diagram we get $A_2 \propto p_\pi/(p_K^2 - m_K^2)$. Noting that the kaon is far off-shell, we see that $A_2 \to 0$, as $p_\pi \to 0$, in the chiral limit. In order to have a consistently systematic expansion in $SU(2)_L \times SU(2)_R$ chiral perturbation theory, we must treat the non-pole and the kaon-pole diagrams as subleading in our calculations, since the amplitudes for the leading order diagrams in Figs. (4.1) and (4.2) do not vanish in the chiral limit.

We need expressions for $\langle K^*|\bar{s}\gamma^\mu(1-\gamma_5)c|D^*\rangle$ and $\langle K^*|\bar{s}\gamma^\mu(1-\gamma_5)c|D\rangle$, in order

to write down the amplitude for the decay. We write [34]

$$\langle K^*(p',\varepsilon')|V_\mu|D(p)\rangle \equiv ig\epsilon_{\mu\nu\lambda\sigma}\varepsilon^{*\prime\nu}(p+p')^\lambda(p-p')^\sigma \tag{4.32}$$

and

$$\langle K^*(p',\varepsilon')|A_\mu|D(p)\rangle \equiv f\varepsilon^{*\prime}_\mu + a^{(+)}(\varepsilon^{*\prime}\cdot p)(p+p')_\mu + a^{(-)}(\varepsilon^{*\prime}\cdot p)(p-p')_\mu, \tag{4.33}$$

where $p'$ and $\varepsilon'$ are the four-momentum and the polarization of the $K^*$, $p$ is the four-momentum of the $D$, $V_\mu \equiv \bar{s}\gamma_\mu c$, $A_\mu \equiv \bar{s}\gamma_\mu\gamma_5 c$, and $g, f, a^{(+)}$, and $a^{(-)}$ are experimentally measurable form factors which are functions of $p\cdot p'$. At the present time, $a^{(-)}$, having a contribution to $D\to K^*\bar{\ell}\nu_\ell$ that is proportional to the lepton mass, remains unmeasured, but $g, f$, and $a^{(+)}$ have been measured [32]. Let $p = m_D v$ and $p' = m_{K^*}v'$, where $v$ and $v'$ are the four-velocities of the $D$ and the $K^*$, respectively. Then, as a function of $y \equiv v\cdot v'$, we have [35]

$$f(y) = \frac{1.8\text{ GeV}}{1+0.63(y-1)}, \tag{4.34}$$

$$a^{(+)}(y) = -\frac{0.17\text{ GeV}^{-1}}{1+0.63(y-1)}, \tag{4.35}$$

and

$$g(y) = \frac{0.51\text{ GeV}^{-1}}{1+0.96(y-1)}. \tag{4.36}$$

Note that the sign of $g$ depends on the convention for the sign of Levi-Civita tensor, which we take to be $\epsilon_{\mu\nu\lambda\sigma} = -\epsilon^{\mu\nu\lambda\sigma} = 1$.

Next, we will write an expression for $\langle K^*|\bar{s}\gamma_\mu(1-\gamma_5)c|D^*\rangle$, in terms of the form factors $g, f, a^{(+)}$, and $a^{(-)}$. Later on, we will only consider the region of phase space where $\bar{K}^{*0}$ is nearly at rest in the decaying $D^0$ rest frame and the dependence of the

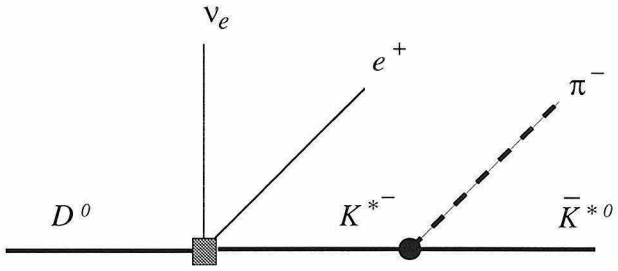


Figure 4.2: The $K^*$-pole diagram contribution to the amplitude in Eq. (4.41). The solid square represents the hadronic left-handed current and the solid circle represents the $K^*K^*\pi$ coupling proportional to $g_2^{(K^*)}$.

amplitude on the unknown form factor $a^{(-)}$ is negligible. We treat the charm quark as heavy and use heavy quark symmetry to write down the following expression [28] for the current $\langle K^*|V_\mu - A_\mu|M^{(H)}\rangle$, where $M^{(H)}$ is either a $D$ or a $D^*$ with polarization $\varepsilon$

$$\langle K^*|V_\mu - A_\mu|M^{(H)}\rangle = \mathrm{Tr}\left[K^*(v,v',\varepsilon')\gamma_\mu(1-\gamma_5)M^{(H)}(v)\right]. \tag{4.37}$$

In Eq. (4.37),

$$M^{(H)}(v) = \frac{1+\not{v}}{2}\begin{cases} -\gamma_5 & ; \text{ for } D \\ \not{\varepsilon} & ; \text{ for } D^*, \end{cases} \tag{4.38}$$

and

$$K^*(v,v',\varepsilon') = (C_1 + C_2\ \not{v}')\ \not{\varepsilon}^{*\prime} + (C_3 + C_4\ \not{v}')(\varepsilon^{*\prime}\cdot v) \tag{4.39}$$

is the most general form that can be written down for the wavefunction of $K^*$, consistent with heavy quark symmetry for $M^{(H)}(v)$, at the leading order. $C_i, i = 1,2,3,4$, are form factors which can be expressed in terms of $f, a^{(+)}, a^{(-)}$, and $g$, by comparing the expression for $\langle K^*|V_\mu - A_\mu|D\rangle$ from Eqs. (4.32) and (4.33) with the one given by Eq. (4.37) above. With the $C_i$ determined in this way, Eq. (4.37) yields the following

expression for $\langle K^*|V_\mu - A_\mu|D^*\rangle$, in terms of the form factors of $\langle K^*|V_\mu - A_\mu|D\rangle$

$$\langle K^*(v',\varepsilon')|V_\mu - A_\mu|D^*(v,\varepsilon)\rangle = m_D m_{K^*}\Bigg(i\epsilon_{\mu\nu\lambda\sigma}\varepsilon^\nu\Bigg[(a^{(+)}-a^{(-)})v^\lambda v'^\sigma(\varepsilon^{*\prime}\cdot v)$$
$$-\frac{f}{m_D m_{K^*}}\varepsilon^{*\prime\lambda}v^\sigma\Bigg] + \Bigg[\frac{f}{m_D m_{K^*}} + \frac{m_D}{m_{K^*}}(a^{(+)}+a^{(-)}) + (a^{(+)}-a^{(-)})(v\cdot v')\Bigg](\varepsilon^{*\prime}\cdot v)\varepsilon_\mu$$
$$+2g(\varepsilon\cdot v')\varepsilon^{*\prime}_\mu + \Bigg\{2g\Big[i\epsilon^{\alpha\beta\gamma\delta}\varepsilon_\alpha v_\beta\varepsilon^{*\prime}_\gamma v'_\delta + (\varepsilon\cdot\varepsilon^{*\prime})(v\cdot v') - (\varepsilon\cdot v')(\varepsilon^{*\prime}\cdot v)\Big]$$
$$-(a^{(+)}-a^{(-)})(\varepsilon\cdot v')(\varepsilon^{*\prime}\cdot v) - \frac{f}{m_D m_{K^*}}(\varepsilon\cdot\varepsilon^{*\prime})\Bigg\}v_\mu - 2g(\varepsilon\cdot\varepsilon^{*\prime})v'_\mu\Bigg), \tag{4.40}$$

where we have used the identity $\varepsilon_\alpha\varepsilon^{*\prime}_\beta v'_\gamma v_\lambda v_\sigma g^{\lambda[\sigma}\epsilon^{\alpha\beta\gamma\mu]} = 0$, to write down the first term proportional to $v_\mu$.

We see that the expressions for $\langle K^*|V_\mu - A_\mu|D\rangle$ and $\langle K^*|V_\mu - A_\mu|D^*\rangle$, given by Eqs. (4.32), (4.33), and (4.40) depend on the value of $a^{(-)}$, which, as mentioned before, is not measured. The value of this form factor could, in principle, be measured, given enough data on $D \to K^*\mu^+\nu_\mu$, where the anti-muon is massive enough to make the measurement possible. However, for the rest of this chapter, we work in the kinematic regime where $\bar{K}^{*0}$ is at rest, to leading order in our calculations, in the rest frame of the decaying $D^0$. Thus, the pion can be soft in the rest frames of both the $D^0$ and the $\bar{K}^{*0}$, as required by chiral perturbation theory. In this region, we have $v = v'$, $v\cdot v' = 1$, and $\varepsilon\cdot v' = \varepsilon^{*\prime}\cdot v = 0$. The amplitude for the decay $D^0 \to \bar{K}^{*0}\pi^- e^+\nu_e$, at leading order in $SU(2)_L \times SU(2)_R$ chiral perturbation theory, represented by Feynman diagrams of Figs. (4.1) and (4.2), is given by

$$\mathcal{M}(D^0 \to \bar{K}^{*0}\pi^- e^+\nu_e) = \frac{G_F V_{cs} f}{\sqrt{2}f_\pi}\Bigg\{\frac{g_D}{v\cdot p_\pi + \Delta}\Big[\epsilon^{\mu\nu\lambda\sigma}v_\nu p_{\pi\lambda}\varepsilon^{*\prime}_\sigma - i(p_\pi\cdot\varepsilon^{*\prime})v^\mu\Big]$$

$$+\frac{g_2^{(K^*)}}{v\cdot p_\pi + i(\Gamma^{(K^*)}/2)}\epsilon^{\mu\nu\lambda\sigma}p_{\pi\nu}\varepsilon^{*\prime}_\lambda v_\sigma\Bigg\}\bar{u}_{(\nu)}\gamma_\mu(1-\gamma_5)v_{(e)}, \tag{4.41}$$

where $u_{(\nu)}$ and $v_{(e)}$ are the spinors for the electron neutrino and the positron, respectively. Note that in the recoilless $\bar{K}^{*0}$ limit used here, the dependence of the

amplitude on $a^{(-)}$ is eliminated. We have $f(1) = 1.8$ GeV, from Eq. (4.34) above.

## 4.4 Differential Decay Rate

Before presenting the differential decay rate, let us introduce the following kinematic variables [37, 38]. The invariant mass of the $K^*\pi$ system $m_{K^*\pi}$, where $m_{K^*\pi} \equiv \sqrt{(p' + p_\pi)^2}$, is given by

$$m^2_{K^*\pi} = m^2_{K^*} + m^2_\pi + 2m_{K^*}m_\pi x, \tag{4.42}$$

where

$$x \equiv \frac{v \cdot p_\pi}{m_\pi}. \tag{4.43}$$

The invariant mass of the lepton pair is denoted by $m_{e\nu}$, where $m_{e\nu} \equiv \sqrt{(p_e + p_\nu)^2}$, $p_e$ is the four-momentum of the positron, and $p_\nu$ is the four-momentum of the electron neutrino. The angle formed by the three-momentum of the $\bar{K}^{*0}$ in the $K^*\pi$ center of mass frame and the line of flight of the $K^*\pi$ in the $D^0$ rest frame is denoted by $\theta_K$, and the angle between the positron three-momentum in the $e^+\nu$ center of mass frame and the line of flight of the $e^+\nu$ in the $D^0$ rest frame is denoted by $\theta_e$. The angle $\phi$ is formed by the normals to the $K^*\pi$ and $e^+\nu$ planes in the $D^0$ rest frame. The sense of $\phi$ is from the normal to the $K^*\pi$ plane to that of the $e^+\nu$ plane.

The amplitude given by Eq. (4.41) is obtained in a region where the $\bar{K}^{*0}$ is "near zero recoil," and later we specify a region of phase space that corresponds to this approximation. Using the above kinematic variables, in the limit $m_\pi/m_{K^*} \to 0$, one obtains the following differential decay rate for $D^0 \to \bar{K}^{*0}\pi^- e^+\nu_e$, in a region where

$\bar{K}^{*0}$ is near zero recoil

$$\frac{d^{(5)}\Gamma(D^0 \to \bar{K}^{*0}\pi^- e^+ \nu_e)}{dx\, dm_{e\nu}^2\, d(\cos\theta_K)\, d(\cos\theta_e)\, d\phi} = \frac{G_F^2 |V_{cs}|^2 f^2(1)}{(4\pi)^6 f_\pi^2 m_D^3} \left(\frac{m_\pi}{m_{K^*}}\right)^2 (x^2-1)^{3/2}\sqrt{T_0}$$
$$\times \left\{ \frac{g_D^2}{(x+\delta)^2}(T_1+T_2) + \left[\frac{g_2^{(K^*)^2}}{x^2+\gamma^2} + \frac{2x\, g_D\, g_2^{(K^*)}}{(x+\delta)(x^2+\gamma^2)}\right] T_2 \right\}, \tag{4.44}$$

where

$$\gamma \equiv \frac{\Gamma^{(K^*)}}{2m_\pi} \quad ; \quad \delta \equiv \frac{\Delta}{m_\pi}, \tag{4.45}$$

$$T_0 \equiv (m_D^2 + m_{K^*}^2 - m_{e\nu}^2)^2 - 4m_D^2 m_{K^*}^2, \tag{4.46}$$

$$T_1 \equiv X^2 \sin^2\theta_e, \tag{4.47}$$

$$\begin{aligned} T_2 \;&\equiv\; \sin^2\theta_K \sin^2\theta_e (X^2 + m_{K^*}^2 m_{e\nu}^2 \cos^2\phi) + m_{K^*}^2 m_{e\nu}^2 (1 + \cos^2\theta_K \cos^2\theta_e) \\ &-\; \left(\frac{m_{K^*} m_{e\nu}}{2}\right) \sin(2\theta_K)\sin(2\theta_e)\cos\phi \sqrt{X^2 + m_{K^*}^2 m_{e\nu}^2}\,, \end{aligned} \tag{4.48}$$

and

$$X \equiv \sqrt{\frac{(m_D^2 - m_{K^*}^2 - m_{e\nu}^2)^2}{4} - m_{K^*}^2 m_{e\nu}^2}\,. \tag{4.49}$$

We can integrate the expression in Eq. (4.44) for the differential decay rate, in order to obtain a total decay rate $\Gamma(D^0 \to \bar{K}^{*0}\pi^- e^+ \nu_e)$, for a limited volume of phase space consistent with the regime of validity of chiral perturbation theory and the recoilless $\bar{K}^{*0}$ approximation. In this region of phase space, we demand that

(a) $p \cdot p_\pi / m_D \ll \Lambda_{\chi B}$ and $p' \cdot p_\pi / m_{K^*} \ll \Lambda_{\chi B}$, where $\Lambda_{\chi B} \sim 1$ GeV, in order to have a valid perturbative expansion, and

(b) $\left|\vec{p'}\right| / m_{K^*} \ll 1$, where $\vec{p'}$ is the three-momentum of the $\bar{K}^{*0}$, in the rest frame of

the $D^0$, to ensure that we stay in a region of phase space where $v = v'$, corresponding to a recoilless $\bar{K}^{*0}$, at leading order.

The constraints in (a) and (b) above are not very exact and an appropriate choice for the region of phase space that satisfies our requirements may, in principle, be made only after comparing the shapes of different distributions from experimental data with the predictions from the theoretical differential decay rate presented in Eq. (4.44). The possibility of making such comparisons between experimental data and our theory depends on the availability and resolution of the data in the restricted phase space region of our calculations.

However, we proceed to make a reasonable choice for the region of integration, given the constraints mentioned in (a) and (b) above. To satisfy $p' \cdot p_\pi / m_{K^*} \ll \Lambda_{\chi B}$, we require $x \in [1, 2]$. The quantities $p \cdot p_\pi / m_D$ and $\left|\vec{p'}\right|$ depend on the values of the variables $x$, $m_{e\nu}$, and $\cos\theta_K$, as shown in the appendix. By inspection, for $x \in [1, 1.5]$, $\cos\theta_K \in [-1, 1]$, and $m_{e\nu}^2 \in [0.593, (m_D - m_{K^*\pi})^2]$, we have $p \cdot p_\pi / m_D < 200$ MeV and $\left|\vec{p'}\right| < 240$ MeV. Integrating the expression in Eq. (4.44) over $m_{e\nu}^2 \in [0.593, (m_D - m_{K^*\pi})^2]$, $x \in [1, 1.5]$, $\cos\theta_K \in [-1, 1]$, $\cos\theta_e \in [-1, 1]$, and $\phi \in [0, 2\pi]$, yields the partial decay width $\Gamma_1(D^0 \to \bar{K}^{*0}\pi^- e^+ \nu_e)$, and

$$\Gamma_1(D^0 \to \bar{K}^{*0}\pi^- e^+ \nu_e) = 9.01 \times 10^{-17}\Big[(0.016)g_D^2 \pm (0.024)g_D + 0.013\Big] \text{ GeV} , \tag{4.50}$$

where $\pm$ corresponds to $g_2^{(K^*)} = \pm 0.6$. With the angular limits of integration the same, if we assume that, without exceeding the realm of validity of our theory considerably, the region of integration may be expanded to $x \in [1, 2]$ and $m_{e\nu}^2 \in [0.510, (m_D - m_{K^*\pi})^2]$, where $p \cdot p_\pi / m_D < 245$ MeV and $\left|\vec{p'}\right| < 330$ MeV, we obtain a partial decay width $\Gamma_2(D^0 \to \bar{K}^{*0}\pi^- e^+ \nu_e)$, which is nearly an order of magnitude larger

$$\Gamma_2(D^0 \to \bar{K}^{*0}\pi^- e^+ \nu_e) = 9.01 \times 10^{-17}\Big[(0.176)g_D^2 \pm (0.231)g_D + 0.117\Big] \text{ GeV} , \tag{4.51}$$

where, again, $\pm$ corresponds to $g_2^{(K^*)} = \pm 0.6$. We mentioned before that present

data suggests $g_D^2 < 0.45$. Let us take $g_D^2 = 0.3$ in order to get some estimates on the size of the branching ratio in our region of phase space. Since the total width $\Gamma_{D^0} = 1.586 \times 10^{-12}\text{GeV}$ for the $D^0$, $\Gamma_1$ gives a branching ratio $B_1$

$$B_1(D^0 \to \bar{K}^{*0}\pi^- e^+ \nu_e) = \begin{cases} 2 \times 10^{-6} & ; \; g_D g_2^{(K^*)} > 0 \\ 3 \times 10^{-7} & ; \; g_D g_2^{(K^*)} < 0, \end{cases} \tag{4.52}$$

in a region where $m_{e\nu}^2 \in [0.593, (m_D - m_{K^*\pi})^2]$ and $x \in [1, 1.5]$. For the branching ratio $B_2$, corresponding to $\Gamma_2$, we get

$$B_2(D^0 \to \bar{K}^{*0}\pi^- e^+ \nu_e) = \begin{cases} 2 \times 10^{-5} & ; \; g_D g_2^{(K^*)} > 0 \\ 3 \times 10^{-6} & ; \; g_D g_2^{(K^*)} < 0 \end{cases} \tag{4.53}$$

in our restricted region of phase space, where $m_{e\nu}^2 \in [0.510, (m_D - m_{K^*\pi})^2]$ and $x \in [1, 2]$. For the smaller value of $B_1$, the corresponding region can most likely be explored at a fixed target experiment, or a $\tau$-charm or $B$ factory only, since the present experiments are not able to measure such small branching ratios for the decay of the $D^0$. However, the values of $B_2$ lie reasonably close to the present measurable range, and $g_D$ can be extracted from the data if its absolute value is not too much smaller than $\sqrt{0.3}$.

Here, we note that the 1-loop calculations of Ref. [31] provide an extraction of $g_D$, using the recent measurement of the branching ratio for $D^{*+} \to D^+\gamma$ [36]. The values that are obtained in Ref. [31] are $g_D = 0.27$ and $g_D = 0.76$. We note that the experimental bound on $D^{*+} \to D^0\pi^+$ suggests that the value $g_D = 0.76$ is excluded. Taking $g_D = 0.27$ and using Eqs. (4.50) and (4.51), we get

$$B_1(D^0 \to \bar{K}^{*0}\pi^- e^+ \nu_e) = \begin{cases} 1 \times 10^{-6} & ; \; g_2^{(K^*)} > 0 \\ 4 \times 10^{-7} & ; \; g_2^{(K^*)} < 0 \end{cases} \tag{4.54}$$

and

$$B_2(D^0 \to \bar{K}^{*0}\pi^- e^+ \nu_e) = \begin{cases} 1 \times 10^{-5} & ; \; g_2^{(K^*)} > 0 \\ 4 \times 10^{-6} & ; \; g_2^{(K^*)} < 0, \end{cases} \tag{4.55}$$

respectively, for the two corresponding kinematic regimes. Hence, Eqs. (4.54) and (4.55) can be viewed as our predictions for the branching ratios of $D^0 \to \bar{K}^{*0}\pi^- e^+ \nu_e$ in the two kinematics regimes, given the value $g_D = 0.27$ of Ref. [31]. On the other hand, a measurement of the $D^0 \to \bar{K}^{*0}\pi^- e^+ \nu_e$ branching ratio, over our regions of integration, can provide an independent extraction of $g_D$.

## 4.5 Summary and Remarks

In this chapter, we have presented a systematic calculation of the differential decay rate for $D^0 \to \bar{K}^{*0}\pi^- e^+ \nu_e$, in a restricted kinematic region, based on the $SU(2)_L \times SU(2)_R$ chiral perturbation theory formalism. Since this decay rate depends on the unmeasured $DD^*\pi$ coupling constant $g_D$ of Eq. (4.12), one can use our results to extract $g_D$ from experimental data. Currently, there is an experimental bound, $g_D^2 < 0.45$, on this coupling constant.

We have treated $D$, $D^*$, and $K^*$ as heavy matter fields and applied the chiral perturbation theory formalism to describe the strong couplings of the $\pi^-$ to $D$, $D^*$, and $K^*$, assuming that the $\pi^-$ is "soft" in the rest frames of the heavy matter fields. The leading order (one derivative here) amplitude involves $\langle K^*|\bar{s}\gamma_\mu(1-\gamma_5)|D\rangle$ and $\langle K^*|\bar{s}\gamma_\mu(1-\gamma_5)|D^*\rangle$ left-handed hadronic currents, and we have presented an expression, in Eq. (4.40), for the $D^* \to K^*$ current, in terms of the form factors of the $D \to K^*$ current. One of the $D \to K^*$ form factors, denoted by $a^{(-)}$, remains unmeasured. However, we have restricted our phase space to a region where the $\bar{K}^{*0}$ is near zero recoil in the $D^0$ rest frame, making the dependence of the amplitude on $a^{(-)}$ negligible, at the leading order. Note that this restriction on the phase space is made in accordance with the requirement that the pion be soft in the rest frames of both the $D^0$ and the $\bar{K}^{*0}$, in order to have a valid chiral perturbation theory expansion.

We have presented an expression for the differential decay rate, in the aforementioned region of phase space, in Eq. (4.44). To get the branching ratio in this region, one has to make a reasonable choice for the limits of the integration that yields the partial width in the restricted volume of phase space. For $|g_D| = \sqrt{0.3}$ as an allowed value for the magnitude of the $DD^*\pi$ coupling, we get the branching ratios, $B_1$ and $B_2$, corresponding to two reasonable choices for the integration region. The first choice is expected to be strict enough for a good leading order approximation, and it can probably be explored at a fixed target experiment, or a $\tau$-charm or $B$ factory only. We believe that expanding the region of integration beyond that which corresponds to the second choice can result in a considerable departure from the proper regime for our approximations. The branching ratios in this region are close to the present measurable range. For a rough extraction of the value of $g_D$ from experiment, we can choose a region of integration for which the branching ratio is of order $10^{-5}$. The volume of phase space in which our theory is valid may be best selected after consulting the data. However, the values of $B_2$ suggest that for a volume of phase space that is close to our second choice presented here, and provided that $|g_D|$ is not too much smaller than the value we used, $\sqrt{0.3}$, an experimental value for $g_D$ can be extracted, using the data on $D^0 \to \bar{K}^{*0}\pi^- e^+ \nu_e$, and given the sign of $g_2^{(K^*)}$. In the heavy quark limit ($m_Q \to \infty$), $g_D$ is equal to $g$ in Eq. (12) of Ref. [26].

There are other processes, with fewer final state particles, that involve the constant $g_D$. $D^* \to D\pi$ is an example of such a process, where one, in principle, can measure the value of $g_D$ from the knowledge of the partial width for this decay channel. This assumes knowing the full width of $D^*$, which is difficult to measure, since the $D^*$ is too short lived for time of flight measurements, and too narrow for a reliable measurement of its full width. However, one can use information on other channels to extract $g_D$, as done in Ref. [31], where recent data on $D^{*+} \to D^+\gamma$ [36] have been used to get $g_D = 0.27$ and $g_D = 0.76$. We note that only the smaller value is consistent with present experimental bounds. Taking $g_D = 0.27$, we obtain, from our results, predictions for the branching ratios of $D^0 \to \bar{K}^{*0}\pi^- e^+ \nu_e$ in two kinematic regimes, where chiral perturbation theory is valid. Alternatively, given data on the above

decay, we can use the results of this chapter to extract the value of $g_D$ independently.

Our results represent the $SU(2)_L \times SU(2)_R$ chiral perturbation theory predictions at the level of one derivative, corresponding to $\mathcal{O}(v_H \cdot p_\pi/1\text{GeV})$, where $v_H$ is the four-velocity of the $D^0$ or $\bar{K}^{0*}$. Thus, we expect to have significant corrections to our results at the level of two derivatives, suppressed by one power of $v_H \cdot p_\pi/1\text{GeV}$, only. Hence, at the next to leading order, operators containing two derivatives of the pion field, insertions of the light quark mass terms, non-pole diagrams, and additional pole diagrams, such as the one in which the $K^{-*}$ is replaced by a $K^-$ in Fig. (4.2), contribute.

# Appendix

The following relations [37] are useful in calculating the scalar products of the various four-vectors introduced in this chapter. Let

$$R \equiv p' + p_\pi \quad ; \quad Q \equiv p' - p_\pi$$

$$K \equiv p_e + p_\nu \quad ; \quad L \equiv p_e - p_\nu. \tag{4.56}$$

We then get

$$Q \cdot R = m_{K^*}^2 - m_\pi^2$$

$$K \cdot L = 0$$

$$R \cdot K = \frac{m_D^2 - m_{K^*\pi}^2 - m_{e\nu}^2}{2}$$

$$\left|\vec{k}\right|^2 \equiv \frac{(m_{K^*}^2 + m_\pi^2 - m_{K^*\pi}^2)^2}{4m_{K^*\pi}^2} - \frac{m_{K^*}^2 m_\pi^2}{m_{K^*\pi}^2}$$

$$\beta = \frac{2\left|\vec{k}\right|}{m_{K^*\pi}}$$

$$\chi = \sqrt{(R \cdot K)^2 - m_{K^*\pi}^2 m_{e\nu}^2}$$

$$K \cdot Q = \frac{m_{K^*}^2 - m_\pi^2}{m_{K^*\pi}^2} R \cdot K + \beta\chi \cos\theta_K$$

$$R \cdot L = \chi \cos\theta_e$$

$$Q \cdot L = \left(\frac{m_{K^*}^2 - m_\pi^2}{m_{K^*\pi}^2}\right) \chi \cos\theta_e + \beta(R \cdot K) \cos\theta_K \cos\theta_e - \beta m_{K^*\pi} m_{e\nu} \sin\theta_K \sin\theta_e \cos\phi$$

$$2\eta \equiv p_D \cdot R = \frac{m_D^2 + m_{K^*\pi}^2 - m_{e\nu}^2}{2}$$

$$2\zeta \equiv p_D \cdot Q = (m_{K^*}^2 - m_\pi^2)\left(1 + \frac{R \cdot K}{m_{K^*\pi}^2}\right) + \beta\chi \cos\theta_K. \tag{4.57}$$

In the above, $p_D$ denotes the four-momentum of the $D^0$. Also, in the limit where $(m_\pi/m_{K^*}) \to 0$, we have $\chi \to X$, where $X$ is defined in Eq. (4.49).

We have the following expressions for the magnitude of the $\bar{K}^{*0}$ three-momentum and the energy of the $\pi^-$, in the rest frame of the $D^0$, denoted by $\left|\vec{p'}\right|$ and $E_\pi$, respectively

$$\left|\vec{p'}\right| = \sqrt{\left(\frac{\eta + \zeta}{m_D}\right)^2 - m_{K^*}^2}$$

$$E_\pi = \frac{\eta - \zeta}{m_D}. \tag{4.58}$$

# Chapter 5 Non-linear Sigma Model Solutions for the Disoriented Chiral Condensate at $\mathcal{O}(p^4)$

## 5.1 Introduction

In chapter 2, we showed that the QCD Lagrangian for strong interactions is invariant under global $SU(N_f)_L \times SU(N_f)_R$ chiral transformations, where $N_f$ is the number of massless flavors. However, as mentioned before, the non-zero masses of quarks in the Standard Model explicitly break this global symmetry. In addition, chiral symmetry is dynamically broken at a scale $\Lambda_{\chi B} \sim 1$ GeV where the vacuum expectation value of the quark bilinear $\langle \bar{q}^i q_j \rangle$ becomes non-zero. Thus, for $N_f$ massless quarks and at energies above $\Lambda_{\chi B}$, the $SU(N_f)_L \times SU(N_f)_R$ symmetry of strong interactions is restored. The restoration of chiral symmetry at non-zero temperatures has been studied in the context of the theory of phase transitions and critical phenomena [39]. According to universality arguments and numerical simulations, in order for the chiral transition to be a second order phase transition, only two quark flavors, namely the up and the down quarks, can be treated as massless [39]. Since the up and the down quark masses are nearly zero compared to the scale of symmetry breaking, the global $SU(2)_L \times SU(2)_R$ is an approximate symmetry of QCD at energy scales above $\Lambda_{\chi B}$.

If the masses of the quarks were zero, the condensate $\langle \bar{q}^i q_j \rangle$ would not have any preferred direction in the vacuum, under $SU(2)_L \times SU(2)_R$. However, the small but non-zero quark masses provide the QCD vacuum with a direction. It has been argued that in certain high energy collisions, such as high energy $\bar{p}p$ [40] or relativistic heavy ion collisions [41, 42, 43, 44], domains of chiral condensates that do not point in the direction of the QCD vacuum may form and grow to a volume of (a few

fermi)$^3$. These domains are referred to as Disoriented Chiral Condensates (DCC's). The eventual decay of DCC's into a large number of pions is predicted to have a distinct experimental signature, namely large fluctuations in the ratio of the number of neutral pions to the total number of pions.

The non-linear sigma model, based on $SU(2)_L \times SU(2)_R$, has the essential features necessary for describing low energy QCD phenomena, and has been used to describe the evolution of the DCC after its formation [41, 42, 43, 45, 46, 47]. In Refs. [43, 46], the authors assume that a relativistic collision can be described by two thin infinite slabs, representing the highly Lorentz-contracted hadrons or nuclei, that collide at the center of mass, and continue along the beam axis in opposite directions. The DCC forms in the region of spacetime between the receding hadrons or nuclei. These authors find boost-invariant (1+1) dimensional classical pion field solutions of the non-linear sigma model at the leading order in a derivative expansion, without the mass term. The solutions they obtain exhibit violent oscillations for small values of the proper time $\tau$, which can be taken as a sign of the breakdown of the formalism at early proper times, where higher order effects become important.

In this chapter, we include the four-derivative terms, ignoring the mass terms, in the Lagrangian for the $SU(2)_L \times SU(2)_R$ non-linear sigma model. We numerically solve the Euler-Lagrange equations to obtain the DCC solutions which are shown to be non-oscillatory at early proper times, $\tau \ll 1/m_\pi$, and we present an analytic explanation for this behavior. We also show that the corrections from terms with four derivatives are important at proper times earlier than about (0.5-0.8) fm. The $\mathcal{O}(p^4)$ solutions for the fields parameterizing the DCC have derivatives that diverge for $\tau \to 0$, as in the case of the previously obtained $\mathcal{O}(p^2)$ solutions. However, the proper times at which the magnitudes of the derivatives are deemed too large for a reliable momentum expansion are smaller than those of the leading order solutions. In the rest of this chapter, by $\mathcal{O}(p^2)$ solutions we mean those obtained from the Lagrangian with terms that have at most two derivatives. The solutions that are obtained from the Lagrangian that contains terms quadratic and quartic in derivatives are referred to as the $\mathcal{O}(p^4)$ solutions.

In the next section, we outline the formalism of the non-linear sigma model at $\mathcal{O}(p^4)$. In Section 5.3, we present the $\mathcal{O}(p^2)$ solutions obtained in Refs. [43, 46]. Section 5.4, where we present our numerical solutions, includes a discussion of our choice of boundary conditions and a comparison of our solutions with those of the leading order. Section 5.5 contains a summary of our results and some concluding remarks.

## 5.2 The Non-linear Sigma Model at $\mathcal{O}(p^4)$

In this section, we establish the formalism used in this chapter to study the evolution of the DCC at the next to leading order in momentum expansion. We use notation similar to that of Ref. [46]. To represent the effects of chiral symmetry breaking and the pion fields, we introduce the fields $\sigma(x)$ and $\vec{\pi}(x)$, respectively. We represent the pion field by

$$\vec{\pi}(x) = f\vec{n}(x)\sin\theta(x), \tag{5.1}$$

where at leading order $f$ is the pion decay constant $f_\pi = 93$ MeV, $\vec{n}$ is a unit isovector field $|\vec{n}|^2 = 1$, and the field $\theta$ is an angle. Note that in this chapter, $f_\pi$ is related to the pion decay constant in the previous chapters via $f_\pi \to f_\pi/\sqrt{2}$. The isovector $\vec{n}$ determines the orientation of the pion field in isospace. The $\sigma$ and $\vec{\pi}$ fields are related by $\sigma^2 + |\vec{\pi}|^2 = f_\pi^2$. We define the field $\Sigma$ by

$$f_\pi\Sigma = \sigma + i\vec{\tau}\cdot\vec{\pi}, \tag{5.2}$$

where $\tau^i$ for $i = 1, 2, 3$ are the Pauli matrices.

The Lagrangian for the non-linear sigma model at $\mathcal{O}(p^2)$, without the mass terms, can then be written as

$$\mathcal{L}^{(2)} = \frac{f_\pi^2}{4}\mathrm{Tr}(\partial_\mu\Sigma\partial^\mu\Sigma^\dagger). \tag{5.3}$$

In terms of the $\theta$ and the $\vec{n}$ fields, we have

$$\mathcal{L}^{(2)} = \frac{f_\pi^2}{2}(\partial_\mu\theta\partial^\mu\theta + \sin^2\theta\ \partial_\mu\vec{n}\cdot\partial^\mu\vec{n}) + \frac{\lambda f_\pi^2}{2}(|\vec{n}|^2 - 1), \tag{5.4}$$

where $\lambda$ is a Lagrange multiplier.

To go to a higher order in the momentum expansion, $\mathcal{O}(p^4)$, we should include operators with four derivatives, or two derivatives and one insertion of the quark mass matrix. However, we continue to ignore the mass terms, since we are mainly interested in the early evolution of the DCC, which corresponds to regions of large momenta. The $\mathcal{O}(p^4)$ contribution $\mathcal{L}^{(4)}$ to the Lagrangian of the system is then given by

$$\mathcal{L}^{(4)} = \beta_1\left[\mathrm{Tr}(\partial_\mu\Sigma\partial^\mu\Sigma^\dagger)\right]^2 + \beta_2\mathrm{Tr}(\partial_\mu\Sigma\partial_\nu\Sigma^\dagger)\mathrm{Tr}(\partial^\mu\Sigma\partial^\nu\Sigma^\dagger), \tag{5.5}$$

where, in the notation of Ref. [48], $\beta_1 = \alpha_1 + \alpha_3/2$, $\beta_2 = \alpha_2$, and $\alpha_i$, $i = 1, 2, 3$, are the coefficients of the $\mathcal{O}(p^4)$ terms for the chiral Lagrangian under $SU(3)_L \times SU(3)_R$ [48]. In terms of $\theta$ and $\vec{n}$, we have for $\mathcal{L}^{(4)}$

$$\begin{aligned}\mathcal{L}^{(4)} &= 4\beta_1\left[(\partial_\mu\theta\partial^\mu\theta)^2 + 2\sin^2\theta\,(\partial_\mu\theta\partial^\mu\theta)\,(\partial_\nu\vec{n}\cdot\partial^\nu\vec{n}) + \sin^4\theta\,(\partial_\mu\vec{n}\cdot\partial^\mu\vec{n})^2\right] \\ &+ 4\beta_2\left[(\partial_\mu\theta\partial^\mu\theta)^2 + \sin^4\theta\,(\partial_\mu\vec{n}\cdot\partial_\nu\vec{n})\,(\partial^\mu\vec{n}\cdot\partial^\nu\vec{n}) + 2\sin^2\theta\,\partial_\mu\theta\partial_\nu\theta\,(\partial^\mu\vec{n}\cdot\partial^\nu\vec{n})\right]\end{aligned} \tag{5.6}$$

The coefficients $\beta_{1,2}$ get renormalized by one-loop diagrams coming from the $\mathcal{O}(p^2)$ Lagrangian, including the mass terms, and are phenomenologically determined. In this chapter, we are only interested in the classical behavior of the pion field, and hence we do not consider the loop effects. As our results represent the qualitative behavior of the DCC, we only give an order of magnitude estimate for the typical size $|\beta|$ of $\beta_1$ and $\beta_2$, and ignore the quantum corrections coming from loop diagrams. We expect this approximation to be qualitatively valid, since by large $N_c$ arguments, where $N_c$ is the number of colors, the effects of loop corrections are suppressed by $N_c^{-1}$.

In order to estimate the $\beta_{1,2}$, we demand, in a systematic momentum expansion

of the Lagrangian

$$\mathcal{L}_p = \left(\frac{f_\pi^2}{4}\right) p^2 + \beta\, p^4 + \mathcal{O}(p^6), \tag{5.7}$$

that all terms be of the same order at the chiral symmetry breaking scale $\Lambda_{\chi B}$. That is,

$$|\beta|\Lambda_{\chi B}^4 \sim \frac{f_\pi^2}{4}\Lambda_{\chi B}^2,$$

and hence

$$|\beta| \sim \frac{f_\pi^2}{4\Lambda_{\chi B}^2}. \tag{5.8}$$

For $f_\pi = 93$ MeV and $\Lambda_{\chi B} = 1$ GeV, we get

$$|\beta| \sim 2 \times 10^{-3}. \tag{5.9}$$

For phenomenologically relevant energy scales, $\beta_1 + \beta_2 > 0$ [48]. Since in the calculations of this chapter it is the combination $\beta_1 + \beta_2$ that appears in the equations of motion, we take $\beta = \beta_1 + \beta_2 > 0$.

## 5.3 The $\mathcal{O}(p^2)$ Solutions

The $\mathcal{O}(p^2)$ Euler-Lagrange equations of motion derived from Eq. (5.4) are given by

$$\partial_\mu \partial^\mu \theta = \sin\theta \cos\theta\, \partial_\mu \vec{n} \cdot \partial^\mu \vec{n} \tag{5.10}$$

and

$$\partial_\mu (\sin^2\theta\, \partial^\mu \vec{n}) = \lambda \vec{n}. \tag{5.11}$$

In Refs. [43, 46], the authors have assumed that the DCC solutions for a relativistic hadronic or nuclear collision have transverse symmetry with respect to the beam di-

rection, where the colliding particles are idealized as two highly Lorentz-contracted slabs of infinite transverse extent. This idealization makes the problem (1+1) dimensional. We take these dimensions to be time $t$ and the beam direction $x$. With the further condition of boost-invariance, the DCC solutions [43, 46] become functions of only proper time $\tau = \sqrt{t^2 - x^2}$, that is $\vec{n} = \vec{n}(\tau)$, and $\theta = \theta(\tau)$. Note that for a function $\phi = \phi(\tau)$ we have $\partial_\mu \phi = (x_\mu/\tau)\phi'$, where a prime denotes a derivative with respect to $\tau$; $\phi' \equiv d\phi/d\tau$. Here, we simply mention the solutions to Eqs. (5.10) and (5.11); the details of the solution are found in Refs. [43, 46].

The angle $\theta$ is given by

$$\cos\theta(\tau) = (b/\kappa)\cos[\kappa \ln(\tau/\tau_0) + \bar{\theta}_0], \tag{5.12}$$

where $\kappa \equiv \sqrt{a^2 + b^2}$, $a \equiv |\vec{a}|$, and $b \equiv |\vec{b}|$; $\vec{a}$ and $\vec{b}$ are two arbitrary constant vectors. In addition, $\cos\bar{\theta}_0 = (\kappa/b)\cos\theta(\tau_0)$, and $\tau_0$ is some arbitrary proper time. The choice of the coordinates in isospace is such that $\vec{a}$, $\vec{c} = \vec{b} \times \vec{a}$, and $\vec{b}$ define a right-handed coordinate system, and $n_a = 0$. We also have

$$n_b(\tau) = (\frac{a}{b})\sqrt{\frac{\kappa^2}{a^2} - \frac{1}{\sin^2\theta(\tau)}}\,. \tag{5.13}$$

The solution for $n_c(\tau)$ is obtained from the constraint $|\vec{n}|^2 = 1$. Here, we take $\cos\theta(\tau_0) = b/\kappa$, implying $\sin\bar{\theta}_0 = 0$ [46], which will make the above solutions (5.12) and (5.13) of the same form as those presented in Ref. [43]. Note that for $a = 0$, we have $\vec{n} =$ Constant as the solution. In the rest of this chapter, we refer to $n_a$, $n_b$, and $n_c$ by $n_1$, $n_2$, and $n_3$, respectively.

The solution for $\theta(\tau)$, given by Eq. (5.12), oscillates rapidly near $\tau = 0$. Small values of $\tau$ correspond to regions in spacetime that are close to the highly energetic nuclei. We expect the theory to break down for small $\tau$, corresponding to large momenta, since our theory is valid only at low momenta. Thus, it may be tempting to interpret $\tau_0$ as a typical proper time below which the theory becomes unreliable [43], as signaled by the "rapid" oscillations. However, the onset of these "rapid"

oscillations is scale-dependent, and cannot reliably determine $\tau_0$, in the above sense.

## 5.4 The $\mathcal{O}(p^4)$ Solutions

In this section, we will show that the solutions to the $\mathcal{O}(p^4)$ equations show no divergent behavior near $\tau = 0$. This does not mean that we can trust the qualitative behavior of the solutions for arbitrarily small $\tau$. Instead, we note that our theory is an expansion in derivatives, and thus we will take the magnitudes of the derivatives of the pion field parameters $\theta$ and $\vec{n}$ to be better indicators of the range of the validity of our solutions. We will thus demonstrate that the $\mathcal{O}(p^4)$ solutions stay reliable down to a length scale of about 0.2 fm.

The Euler-Lagrange equations of motion for $\theta$ and $\vec{n}$ are derived from the Lagrangian $\mathcal{L}$, given by

$$\mathcal{L} = \mathcal{L}^{(2)} + \mathcal{L}^{(4)}, \tag{5.14}$$

where $\mathcal{L}$ includes the derivative terms up to $\mathcal{O}(p^4)$. The equation for $\theta$ is

$$f_\pi^2 \left( \frac{\theta'}{\tau} + \theta'' - \sin\theta\cos\theta|\vec{n}'|^2 \right) + 16(\beta_1+\beta_2)\Bigg[ \left( \frac{\theta'}{\tau} + \theta'' \right) \left( \theta'^2 + \sin^2\theta|\vec{n}'|^2 \right)$$
$$+2\theta'^2\theta'' + 2\sin^2\theta\,\theta'(\vec{n}'\cdot\vec{n}'') + \sin\theta\cos\theta|\vec{n}'|^2 \left( \theta'^2 - \sin^2\theta|\vec{n}'|^2 \right) \Bigg] = 0. \tag{5.15}$$

For $\vec{n}$, we get the following equation

$$f_\pi^2 \left[ 2\cos\theta\,\theta'\,\vec{n}' + \sin\theta \left( \frac{\vec{n}'}{\tau} + \vec{n}'' + |\vec{n}'|^2\vec{n} \right) \right] + 16(\beta_1+\beta_2) \Bigg\{ \sin\theta \Bigg[ 2\theta'\theta''\vec{n}'$$
$$+\theta'^2 \left( \frac{\vec{n}'}{\tau} + \vec{n}'' \right) + 4\sin\theta\cos\theta\,\theta'|\vec{n}'|^2\vec{n}' + \sin^2\theta|\vec{n}'|^2 \left( \frac{\vec{n}'}{\tau} + \vec{n}'' \right)$$
$$+2\sin^2\theta(\vec{n}'\cdot\vec{n}'')\vec{n}' + \left( \sin^2\theta|\vec{n}'|^2 + \theta'^2 \right)|\vec{n}'|^2\vec{n} \Bigg] + 2\cos\theta\,\theta'^3\vec{n}' \Bigg\} = 0, \tag{5.16}$$

where we have used the constraint $\vec{n}\cdot\vec{n}'' = -|\vec{n}'|^2$.

To solve the above coupled non-linear ordinary differential equations (5.15) and

(5.16), we need to specify the boundary conditions. In this chapter, we choose the boundary conditions for the $\mathcal{O}(p^4)$ fields $\theta$ and $\vec{n}$ and their derivatives to be the values of the corresponding $\mathcal{O}(p^2)$ solutions evaluated at a "late" proper time $\tau_l$, where the $\mathcal{O}(p^2)$ and $\mathcal{O}(p^4)$ solutions approximately coincide. We choose $\tau_0 = 1/2m_\pi$, as a typical proper time where we expect the higher order interactions to become important, $\beta_1 + \beta_2 = \beta = 2 \times 10^{-3}$, and $a = b = 1$. We pick $\tau_l = 10\tau_0$. In this way, the solutions of the $\mathcal{O}(p^2)$ equations have definite values at $\tau_l$. Numerically, we have $\tau_0 \approx 0.7$ fm, and $\tau_l \approx 7$ fm, at which we expect the $\mathcal{O}(p^2)$ solutions to approximate the $\mathcal{O}(p^4)$ solutions with good accuracy.

In Figs. (1) through (6), we present our numerical solutions for the fields $\theta$ and $\vec{n}$ and their derivatives. Note that as a result of current conservation relations [46], $n_1 = 0$ and $n_1' = 0$, as in the case of the leading order solutions. Each figure contains the $\mathcal{O}(p^2)$ solution, represented by the dashed line, and the $\mathcal{O}(p^4)$ solution, represented by the solid line. The $\mathcal{O}(p^2)$ solutions are obtained numerically and agree with those of the analytic expressions in Eqs. (5.12) and (5.13).

The solutions presented here are computed for $\tau \in [10^{-6}\text{MeV}^{-1}, 5/m_\pi]$. Figures (1), (2), and (3) show that the rapid oscillations of the $\mathcal{O}(p^2)$ solutions for $\theta$ and $\vec{n}$, near $\tau = 0$, no longer arise in the $\mathcal{O}(p^4)$ solutions, where the inclusion of the higher order terms seems to stabilize the solutions. The $\mathcal{O}(p^4)$ and the $\mathcal{O}(p^2)$ field derivatives presented in Figs. (4), (5), and (6) show divergent behavior near $\tau = 0$. The analytic $\mathcal{O}(p^2)$ solutions of Eqs. (5.12) and (5.13) yield divergent and oscillatory derivatives for $\tau = 0$. We found that the magnitudes of the $\mathcal{O}(p^4)$ derivatives did not stabilize and continued to grow with decreasing $\tau$, without oscillation.

In order to understand the behavior of the $\mathcal{O}(p^4)$ solutions mentioned above, we examine Eq. (5.15) in the limit $\tau \to 0$, for the case of constant $\vec{n}$. The solutions with constant $\vec{n}$ are related to those with spacetime dependence by chiral rotations [46]. In this case, Eq. (5.15) reduces to

$$f_\pi^2 \left( \frac{\theta'}{\tau} + \theta'' \right) + 16(\beta_1 + \beta_2) \left( \frac{\theta'}{\tau} + 3\theta'' \right) \theta'^2 = 0. \tag{5.17}$$

Let us assume that for small $\tau$, the behavior of the field $\theta$ is given by

$$\theta = \tilde{\theta} + \left(\frac{\tau}{\tilde{\tau}}\right)^p, \tag{5.18}$$

where $\tilde{\theta}$ and $\tilde{\tau}$ are constants. We expect to find a solution for $\theta$ with $0 < p < 1$ that tends to a constant $\tilde{\theta}$ but has a divergent derivative, as $\tau \to 0$. Upon substituting the expression in Eq. (5.18) for $\theta$ into Eq. (5.17), we get the following equation:

$$f_\pi^2[p + p(p-1)] + 16(\beta_1 + \beta_2)[p + 3p(p-1)]p^2 \left(\frac{\tau}{\tilde{\tau}}\right)^{2p} \left(\frac{1}{\tau}\right)^2 = 0. \tag{5.19}$$

In the absence of the $\mathcal{O}(p^4)$ terms, we only have the terms proportional to $f_\pi^2$. In this case, we get $p = 0$, which is consistent with the solution $\theta \sim \ln(\tau/\tilde{\tau})$ of the equation $\theta'/\tau + \theta'' = 0$. However, we see that for small $\tau$, the terms proportional to $\beta_1 + \beta_2$ will be dominant if $0 < p < 1$. Thus, for $\tau \to 0$, we ignore the terms proportional to $f_\pi^2$. We then get

$$p = \frac{2}{3}, \tag{5.20}$$

in agreement with our prior assumption that $0 < p < 1$.

The numerical solutions presented here are obtained in the context of a systematic derivative expansion. Thus, it is the magnitudes of the derivatives that establish the region of validity of the solutions. We take the maximum magnitude of the derivative of a field below which the expansion is valid to be $p_{max} \sim 500$ MeV. The graphs in Figs. (4), (5), and (6) show that the magnitudes of the $\mathcal{O}(p^4)$ field derivatives stay below $p_{max}$ for values of $\tau$ down to $\tau = 10^{-3}$ MeV$^{-1} \sim \Lambda_{\chi B}^{-1}$, which is as small a proper time as we can consider in our formalism. In contrast, the magnitudes of the $\mathcal{O}(p^2)$ field derivatives begin to exceed $p_{max}$ at proper times $\tau \lesssim (2-4) \times 10^{-3}$ MeV$^{-1}$, indicating a smaller range of validity for these solutions. Hence, our results suggest that the $\mathcal{O}(p^4)$ solutions can be used to study the qualitative evolution of the DCC down to a length scale of $\sim 0.2$ fm, but the $\mathcal{O}(p^2)$ solutions lose their qualitative

validity below a length scale of $\sim (0.5 - 0.8)$ fm.

## 5.5 Summary and Remarks

In this chapter, we derived the $\mathcal{O}(p^4)$ equations of motion for the DCC produced in an idealized relativistic collision, using the non-linear sigma model Lagrangian without the mass terms. We presented our numerical solutions for the $\mathcal{O}(p^4)$ equations of motion. The higher order corrections to the $\mathcal{O}(p^2)$ solutions are only important for small values of proper time $\tau \ll 1/m_\pi$. Hence, the absence of the mass terms, important only for $\tau \gtrsim 1/m_\pi$, does not introduce significant qualitative changes in the early proper time solutions. Our $\mathcal{O}(p^4)$ solutions for the fields $\theta$ and $\vec{n}$, parameterizing the DCC field configuration, stabilize for small values of proper time, whereas the $\mathcal{O}(p^2)$ solutions oscillate rapidly with decreasing $\tau$. We presented a qualitative explanation for the behavior of the solutions by studying the equations of motion, in a special case and in the limit where $\tau \to 0$.

A measure of the validity of our derivative expansion is the magnitude of the field derivatives. We took $p_{max} \sim 500$ MeV to be the maximum value for the magnitude of a field derivative beyond which the solutions cannot be trusted. Using this criterion, the $\mathcal{O}(p^4)$ solutions were deemed reliable down to $\tau \sim 0.2$ fm, whereas the $\mathcal{O}(p^2)$ solutions were considered no longer qualitatively valid below $\tau \sim (0.5 - 0.8)$ fm. We take our solutions to represent a qualitative measure of the behavior of the DCC. Our results suggest that this qualitative behavior can be studied within the non-linear sigma model down to a length scale of $\sim 0.2$ fm, once the $\mathcal{O}(p^4)$ derivative corrections to the Lagrangian are included. A length scale of $\sim 0.2$ fm corresponds to the energy scale $\Lambda_{\chi B} \sim 1$ GeV, where chiral symmetry is restored and the non-linear sigma model formalism is no longer valid. Hence, we do not expect the inclusion of the higher order terms beyond $\mathcal{O}(p^4)$ in the chiral Lagrangian to enable us to study even earlier proper times in the evolution of the DCC.

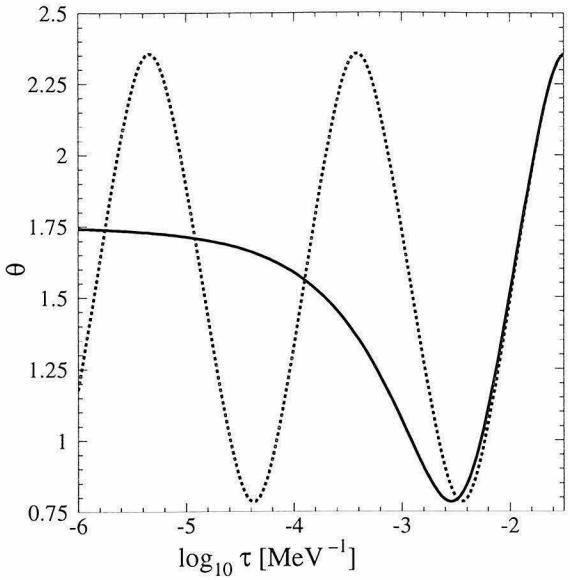


Figure 5.1: The dashed and the solid lines represent the $\mathcal{O}(p^2)$ and the $\mathcal{O}(p^4)$ solutions for $\theta$, respectively. The $\mathcal{O}(p^2)$ solution for $\theta$ oscillates increasingly rapidly with decreasing $\tau$, as Eq. (5.12) implies, while the $\mathcal{O}(p^4)$ solution does not oscillate as $\tau \to 0$. Similar comments apply to the solutions for $n_2$ and $n_3$ in Figs. (5.2) and (5.3), respectively.

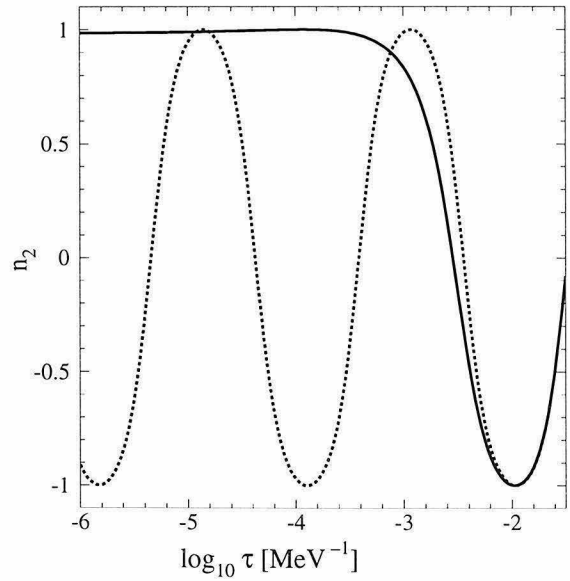


Figure 5.2: The dashed and the solid lines represent the $\mathcal{O}(p^2)$ and the $\mathcal{O}(p^4)$ solutions for $n_2$, respectively.

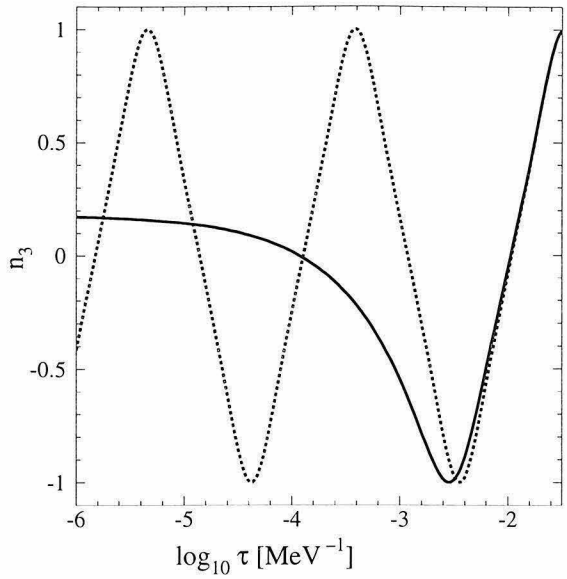


Figure 5.3: The dashed and the solid lines represent the $\mathcal{O}(p^2)$ and the $\mathcal{O}(p^4)$ solutions for $n_3$, respectively.

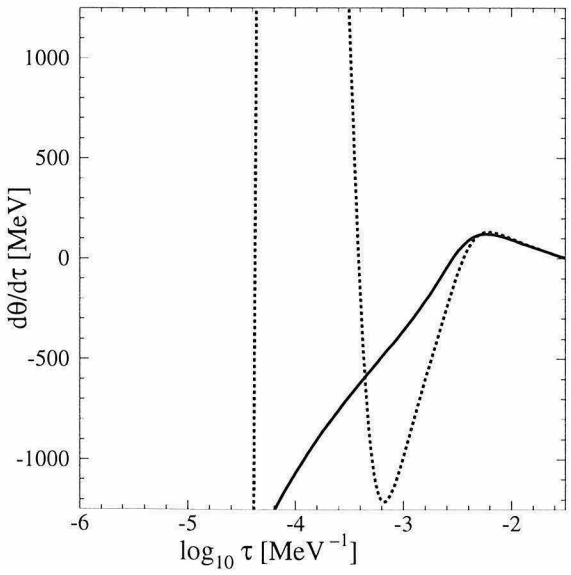


Figure 5.4: The dashed and the solid lines represent the $\mathcal{O}(p^2)$ and the $\mathcal{O}(p^4)$ solutions for $\theta'$, respectively. The $\mathcal{O}(p^2)$ solution for $\theta'$ oscillates and has a divergent magnitude, while the $\mathcal{O}(p^4)$ solution for $\theta'$ diverges in magnitude, but does not oscillate. Similar comments apply to the solutions for $n_2'$ and $n_3'$ in Figs. (5.5) and (5.6), respectively.

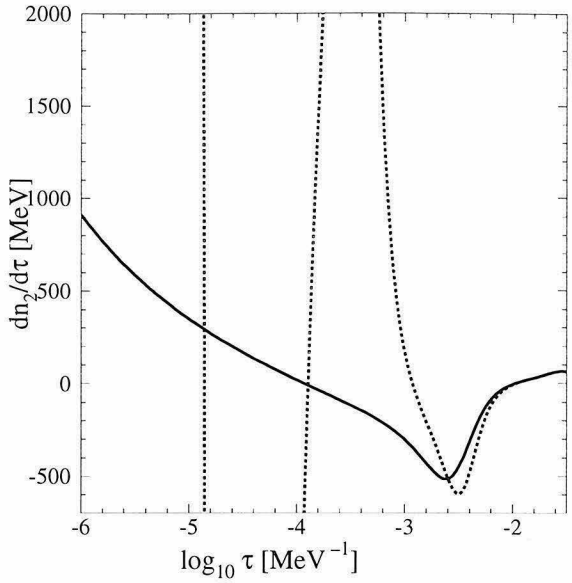


Figure 5.5: The dashed and the solid lines represent the $\mathcal{O}(p^2)$ and the $\mathcal{O}(p^4)$ solutions for $n_2'$, respectively.

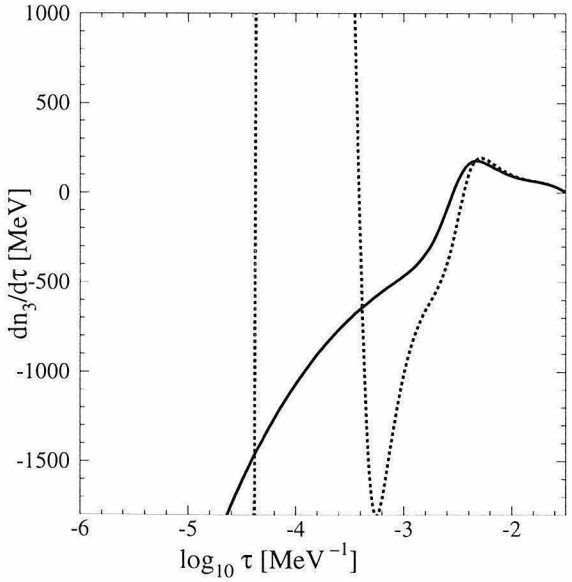


Figure 5.6: The dashed and the solid lines represent the $\mathcal{O}(p^2)$ and the $\mathcal{O}(p^4)$ solutions for $n_3'$, respectively.

# Chapter 6 Conclusion

In this work, we studied how the concepts of global symmetry breaking and generation of Goldstone bosons lead to a systematic method for treating hadronic processes at low energies, where perturbative QCD calculations are not valid. We noted that the quantum mechanical breaking of the approximate chiral symmetry of the classical QCD Lagrangian explains the appearance of the eight lightest pseudo-scalar mesons, the pseudo-Goldstone bosons of the theory.

Using some general arguments, we showed how one could write down an effective chiral Lagrangian for the interactions of the pseudo-scalars which have derivative couplings. Thus, we noted that, at low momenta, the order of the resulting chiral perturbation would be given by the number of derivatives in the terms included in the effective Lagrangian. We also gave a heuristic argument that the scale of chiral symmetry breaking is $\Lambda_{\chi B} \sim 1$ GeV. We later used these ideas as the basis of our approach to three different problems in chapters 3, 4, and 5. In each of these chapters, we appropriately augmented the basic chiral formalism developed earlier in order to treat a certain problem. In the applications considered in this work, we only used chiral $SU(2)_L \times SU(2)_R$ symmetry.

In chapter 3, we introduced heavy vector meson chiral perturbation theory and used it to predict differential decay distributions for $\tau \to V\pi\nu_\tau$, where $V$ is a $\rho$ meson or a $K^*$ meson. We also predicted the rate for $\tau \to \omega\pi\nu_\tau$, and by comparing with experimental data, we determined the value of the $\rho\omega\pi$ coupling constant. In the limit of $SU(3)$ flavor symmetry and large $N_c$, this is the coupling constant $g_2^{(\rho)}$ that determines the strength of the interactions of the vector mesons with the pseudo-scalars in heavy vector meson chiral perturbation theory.

In chapter 4, we studied the decay $D^0 \to \bar{K}^{*0}\pi^- e^+ \nu_e$, using heavy meson and heavy vector meson chiral perturbation theory. The rate for this decay depends on the $DD^*\pi$ coupling constant $g_D$. Using the value of $g_2^{(\rho)}$ from chapter 3, we showed

that an experimental measurement of this decay in a restricted kinematic regime can result in an extraction of the magnitude of $g_D$. We also gave our prediction for the rate of the above decay in this kinematic regime, using a value of $g_D$ that was determined through a different approach.

In chapter 5, we presented boost-invariant (1+1) dimensional solutions for the DCC, obtained numerically, using the non-linear sigma model for the interactions of pions at $\mathcal{O}(p^4)$. We examined the early proper time behavior of the solutions, for which we ignored the mass terms in the Lagrangian. We found that, whereas the $\mathcal{O}(p^2)$ solutions have singular behavior at early proper times, the $\mathcal{O}(p^4)$ solutions did not behave in a singular fashion. We also presented an analytic argument for this non-singular behavior. We noted that our $\mathcal{O}(p^4)$ solutions could be used to present the qualitative behavior of the DCC above a length scale of about 0.2 fm corresponding to a momentum scale of about 1 GeV. Since the chiral expansion breaks down below this length scale, we concluded that going to higher orders in chiral perturbation theory would not enable us to study the DCC at smaller length scales, within the non-linear sigma model.

The uses of chiral symmetry in studying low energy hadronic processes are numerous and diverse. In this work, it was our goal to present a few of the uses of chiral perturbation theory and to show the power and generality of the concepts that were introduced in chapter 2. It is the hope of the author that this work has achieved the aforementioned goal to some degree.

# Bibliography

[1] William Shakespeare, King Henry IV., First Part, *The Complete Works of William Shakespeare*, Gramercy Books.

[2] D.J. Gross and F. Wilczek, Phys. Rev. Lett., **30**, 1343 (1973).

[3] H.D. Politzer, Phys. Rev. Lett., **30**, 1346 (1973).

[4] S. Weinberg, Phys. Rev. Lett. **19**, 1264 (1967); A. Salam, *Elementary Particle Physics*, ed. N. Svartholm, Almqvist and Wiksells, Stockholm (1968).

[5] J. Goldstone, Nuovo Cimento **9**, 154 (1961); J. Goldstone, A. Salam, and S. Weinberg, Phys. Rev. **127**, 965 (1962).

[6] P. Langacker and H. Pagels, Phys. Rev. **D10** 2904 (1974); J. Bijnens, H. Sonoda, and M.B. Wise, Nucl. Phys. **B261** 185 (1985); J. Gasser, M.E. Sainio and A. Svarc, Nucl. Phys. **B307**, 779 (1988); E. Jenkins and A.V. Manohar, Phys. Lett. **B255**, 558 (1991); **259** 353 (1991).

[7] M.B. Wise, Phys. Rev. **D45** 2188 (1992); G. Burdman and J.F. Donoghue, Phys. Lett. **B280** 287 (1992); T.-M. Yan, et.al., Phys. Rev. **D46** 1148 (1992); P. Cho, Nucl. Phys. **B396** 183 (1993).

[8] N. Isgur and M.B. Wise, Phys. Lett. **B232**, 113 (1989); *ibid* **237**, 527 (1990).

[9] H. Davoudiasl and M. B. Wise, Phys. Rev. **D53** 2523 (1996).

[10] H. Davoudiasl, Phys. Rev. **D54**, 6830 (1996).

[11] H. Davoudiasl, Phys. Lett. **B397**, 234 (1997).

[12] Lewis H. Ryder, *Quantum Field Theory*, Cambridge University Press (1992).

[13] A. Pich, Rept. Prog. Phys. **58**, 563 (1995).

[14] M. Gell-Mann, Phys. Rev. **106** 1296 (1957); S. Okubo, Prog. Theor. Phys. **27** 949 (1962).

[15] E. Jenkins, A.V. Manohar and M.B. Wise, Phys. Rev. Lett. **75** 2272 (1995).

[16] G. 't Hooft, Nucl. Phys. **B72** 461 (1974).

[17] R. Balest, et al., (CLEO Collaboration) Phys. Rev. Lett. 75, 3809 (1995).

[18] R. Decker, M. Finkemeier and E. Mirkes, Phys. Rev. **D50** 6863 (1994).

[19] See, for example, J.J.J. Kokkedee, *The Quark Model* (Benjamin, New York 1969). In the same approximation, the pion nucleon coupling $g_A = 5/3$. Experimentally, $g_A \approx 1.25$.

[20] In Fig. (3b) of Ref. [17] the function $v$ is plotted. Using Eq. (3.40) our prediction for the spectral function $v$ as a function of, $x = (m_{\omega\pi}^2 - m_\omega^2 - m_\pi^2)/2m_\pi m_\omega$, is

$$v(x) = \frac{1}{6\pi}\left(\frac{m_\pi}{m_\omega}\right)\left(\frac{f_\rho}{f_\pi}\right)^2 \frac{1}{m_\omega^2}\frac{(x^2-1)^{3/2}}{x^2(1+\gamma^2)} g_2^{(\rho)^2}.$$

Experimentally, the $\rho$ decay constant is $f_\rho \approx (407\text{MeV})^2$. In Fig. (3b), in the first bin, $0.9\text{GeV} < m_{\omega\pi} < 1.0\text{GeV}$, $v = (0.0029 \pm 0.0004)$, and in the second bin $1\text{GeV} < m_{\omega\pi} < 1.1\text{GeV}, v = (0.0156 \pm 0.0018)$. These errors are only statistical.

[21] For a discussion of data on $K\pi\pi$ hadronic final states, see J.G. Smith (CLEO Collaboration) Nucl. Phys. B (Proc. Suppl.) **40** 351 (1995); M. Battle *et al.* (CLEO Collaboration), Phys. Rev. Lett. **73** 1079 (1994). There, it is reported that $Br(\tau \to \bar{K}^0\pi^-\pi^0\nu_\tau) = (0.39 \pm 0.06 \pm 0.06)\%$; $Br(\tau \to K^-\pi^0\pi^0\nu_\tau) = (0.14 \pm 0.1 \pm 0.03)\%$.

[22] S.I. Eidelman and V.N. Ivanchenko, Nucl. Phys. B (Proc. Suppl.) **40** 131 (1995).

[23] A.V. Manohar and H. Georgi, Nucl. Phys. **B234** 189 (1984).

[24] CLEO Collaboration, R. Balest *et al.*, Phys. Rev. Lett. **75**, 3809 (1995).

[25] See H. Georgi, Report No. HUTP-91-A039, 1991 (unpublished).

[26] M. B. Wise, Phys. Rev. **D45**, R2188 (1992).

[27] M. Neubert, Phys. Rep. **245**, 259 (1994).

[28] This approach was brought to my attention by Zoltan Ligeti.

[29] P. Cho and H. Georgi, Phys. Lett. **B296** (1992) 408.

[30] J.F. Amundson *et al.*, Phys. Lett. **B296** (1992) 415.

[31] I.W. Stewart, hep-ph/9803227.

[32] Particle Data Group, Phys. Rev. **D54**, Part I (1996).

[33] G. P. LePage and B. A. Thacker, in *Field Theory on the Lattice*, Proceedings of the International Symposium, Seillac, France, 1987, edited by A. Billoire *et al.* [Nucl. Phys. B (Proc. Suppl.) **4**, 199 (1988)].

[34] N. Isgur *et al.*, Phys. Rev. **D39**, 799 (1989).

[35] Z. Ligeti and M. B. Wise, Phys. Rev. **D53** 4937 (1996).

[36] CLEO collaboration, hep-ex/9711011.

[37] C.L.Y. Lee *et al.*, Phys. Rev. **D46**, 5040 (1992).

[38] A. Pais and S. B. Treiman, Phys. Rev. **168**, 1858 (1968); see also N. Cabibbo and A. Maksymowicz, ibid. **137**, B438 (1965).

[39] R. Pisarski and F. Wilczek, Phys. Rev. **D29**, 338 (1984); F. Wilczek, Int. J. Mod. Phys. **A7**, 3911 (1992); K. Rajagopal and F. Wilczek, Nucl. Phys. **B399** 395 (1993); *ibid.* **404** 577; for a review see K. Rajagopal, *Quark-Gluon Plasma 2*, Editor R. C. Hwa, World Scientific (1995).

[40] J. D. Bjorken, Int. J. Mod. Phys. **A7**, 4189 (1992); J. D. Bjorken, Acta Physica Polonica **B23**, 561 (1992); J. D. Bjorken, K. L. Kowalski, and C. C. Taylor,

*Baked Alaska*, Proceedings of Les Rencontres de Physique de la Vallée D'Aoste, La Thuile, SLAC-PUB-6109 (1993).

[41] A.A. Anselm, Phys. Lett. **B217** 169 (1989).

[42] A.A. Anselm and M. G. Ryskin, Phys. Lett. **B266** (1991) 482.

[43] J. -P. Blaizot and A. Krzywicki, Phys. Rev. **D46** 246 (1992).

[44] K. Rajagopal and F. Wilczek in Ref. [39].

[45] J. -P. Blaizot and A. Krzywicki, Phys. Rev. **D50** 442 (1994).

[46] Z. Huang and M. Suzuki, Phys. Rev. **D53** 891 (1996).

[47] M. Suzuki, Phys. Rev. **D54** 3556 (1996).

[48] J. F. Donoghue, E. Golowich, B. R. Holstein, *Dynamics of the Standard Model*, Cambridge (1994).